REPORT DOCUMENTATION PAGE

AFRL-SR-BL-TR-99-

0036

vis

1. AGENCY USE ONLY (Leave Blank)	2. REPORT DATE	3. RI
	January 29, 1999	Final Report, 15 Aug 97 – 14 Aug 98

4. TITLE AND SUBTITLE
Development of High Temperature Solid Lubricant Coatings

5. FUNDING NUMBERS
F49620-97-C-0054
STTR/TS
65502F

6. AUTHOR(S)
Rabi S. Bhattacharya and Steven Keller

7. PERFORMING ORGANIZATION NAME(S) AND ADDRESS(ES)
UES, Inc.
4401 Dayton-Xenia Road
Dayton OH 45432-1894

8. PEFORMING ORGANIZATION REPORT NUMBER
UES P168

9. SPONSORING/MONITORING AGENCY NAME(S) AND ADDRESS(ES)
United States Air Force
Air Force Office of Scientific Research
110 Duncan Avenue, Room B115
Bolling AFB DC 20332-8050

10. SPONSORING/MONITORING AGENCY REPORT NUMBER

11, SUPPLEMENTARY NOTES

19990218009

12a. DISTRIBUTION/AVAILABILITY STATEMENT
Approved for public release; distribution is unlimited.

12b. DISTRIBUTION CODE
A

13. ABSTRACT *(Maximum 200 words)*

The primary research objective of this work was to develop a solid lubricant coating that can function over a broad temperature range. The approach investigated consisted of developing adaptive lubricant coating from materials that undergo chemical change with increasing temperature by reacting together and with the environment. To test this approach, UES and Cleveland State University have conducted experiments to form cesium oxythiotungstate, a high temperature lubricant, on Inconel 718 surface from composite coatings of cesium tungstate and tungsten sulfide. The coatings were deposited by RF sputtering and characterized by X-ray Photoelectron Spectroscopy (XPS). The results indicate that sulfur escapes from the composite coating upon exposure to temperature above 500°C in air. Thus, the desired adaptive lubricant phase, cesium oxythiotungstate could not be formed. However, cesium oxythiotungstate phase has been found to form upon annealing at high temperature in vacuum. The friction coefficients of sputtered cesium oxythiotungstate and cesium tungstate coatings have been measured.

14. SUBJECT TERMS
Cesium oxythiotungstate, sputtering, cesium tungstate, dry lubricant, tungsten disulfide, solid lubricant

15. NUMBER OF PAGES

16. PRICE CODE

17. SECURITY CLASSIFICAITON OF REPORT	18. SECURITY CLASSIFICATION OF THIS PAGE	19. SECURITY CLASSIFICATION OF ABSTRACT	20. LIMITATION OF ABSTRACT
Unclassified	Unclassified	Unclassified	UL

NSN 7540-01-280-5500

Standard Form 298 (Rev 2-89)
Prescribed by ANSI Std. 239-18
298-102

PREFACE

This technical report has been prepared as part of the requirement of the Phase I STTR Contract No.F49620-97-C-0054 with the United State Air Force, Air Force Office of Scientific Research, Bolling AFB, DC. The report covers work conducted during the period 15 August 1997 through 14 August 1998, and constitutes the final report under the contract.

TABLE OF CONTENTS

LIST OF FIGURES

1.0 INTRODUCTION

Advanced turbine engines operating at high temperatures need lubricants that are functional over a broad temperature range, -50°C to 1000°C. The benefits of operating engines at a higher operating temperature include improved thermodynamic efficiency resulting in better engine power to weight ratio and improved fuel efficiencies. The primary barrier to successful high temperature engine development, however, is the limited capability of available lubricants to enhance the performance and durability of critical engine components. Liquid lubricants can't be used because of thermal and oxidative degradation at high temperatures above about 300°C. Therefore, suitable solid lubricants are needed that can function over a wide range of temperatures.

The maximum useful temperature for most common solid lubricants such as MoS_2, WS_2 etc., are limited to about 400°C under favorable conditions in air atmosphere [1]. In vacuum applications, however, these materials can be used at higher temperatures (~600°C).

The other common lubricant is graphite which requires the presence of water or hydrocarbons to develop good lubricating properties. Graphite lubricates at room temperature and above 425°C but not at intermediate temperatures. Low friction at room temperature is attributed to the beneficial effect of absorbed moisture. High friction at intermediate temperature is attributed to desorption of water and possibly other gases. Low friction above 425°C is attributed to interaction of graphite with oxides of the lubricated metal. Graphite itself begins to oxidize at about 400°C. The graphite fluoride, $(CF_x)n$, is a layer lattice compound of graphite and a good lubricant. However, the thermal decomposition limits its applications up to 480°C.

Over the years, some unconventional solid lubricants based on oxides and fluorides have been identified for high temperature applications [2,3]. These are: MoO_3, TiO_x, CoO, ZnO, ZrO_2, LiF, CaF_2, BaF_2. Use of oxides and fluorides has been limited because of their lubricating ability within a narrow temperature range. Also, the friction coefficient of most of these oxides even at high temperatures is rather high, ~0.2-0.4.

The objective of this work was to develop solid lubricant coatings that can function over a broad temperature range in air atmosphere.

2.0 BACKGROUND

A new class of materials belonging to complex metal chalcogenides have recently been identified for high temperature applications [4]. These complex chalcogenides can be represented by the following general formula:

$$M_aM_b{}^1O_cS_d$$

where M = different metals
M^1 = Molybdenum or Tungsten

O = Oxygen
S = Sulfur

Two compositions, in particular, have shown superior thermal, oxidative and tribological properties over a broad temperature range up to 650°C. These are: cesium oxytrithiotungstate and zinc oxytrithiomolybdate. The friction coefficients reported so far using these lubricants are in the range 0.15 - 0.37 depending on the temperature. Usually higher friction coefficient was found at lower temperature. These lubricants apparently degrade at temperatures greater than 650°C. These complexes may be synthesized in the form of coatings by using co-sputtering of suitable components and subsequent heat treatment.

UES, Inc. and Cleveland State University (CSU) proposed to develop a solid lubricant coating that can function over a broad temperature range. The approach was to develop adaptive lubricant coatings from materials that undergo chemical change with increasing temperature by reacting together and with the environment. Specifically, in Phase I, we proposed to study composite coatings made from cesium tungstate (Cs_2WO_4) and WS_2. WS_2 provides low friction in air up to about 450°C. As the temperature increases, WS_2 may react with cesium tungstate in air to form cesium oxythiotungstate (Cs_2WOS_3) which exhibits low friction at high temperature (650°C). Addition of CaF_2 may increase its lubricating capability up to 850°C.

3.0 PHASE I EXPERIMENTAL PROGRAM

The Phase I experimental program consisted of establishing conditions for depositing composite films of WS_2 and Cs_2WO_4 using sputtering. X-ray photoelectron spectroscopy (XPS) was used to analyze the composition and chemical states of the coating material before and after annealing at various temperatures. Friction and wear characteristics of these coatings at room and elevated temperatures were evaluated by using a pin-on-plate machine at CSU.

The questions addressed in Phase I include: (a) Can the low friction cesium oxythiotungstate form from a mixed WS_2 and Cs_2WO_4 film as the temperature increases?; (b) How do the composition, chemistry and microstructure of the coating influence the friction and wear behavior?

3.1 EXPERIMENTAL PROCEDURE

3.1.1 Preparation of Cs_2WO_4 and Cs_2WOS_3 Sputter Targets

Cs_2WO_4 target: The Cs_2WO_4 target was fabricated using standard sinter process at Superconductive Components Inc. (SCI) in Columbus, OH. Cs_2WO_4 powders, which was produced by calcining a mixture of Cs_2CO_3 and WO_3, was first pressed uniaxially in a 2.5 inch die under a pressure of 10,000 lbs. The pressed part was then isostatically pressed at 5000 psi using Ar gas and was sintered for 6 hrs at temperatures between 625-675°C. The target was then machined to a diameter of 2" and thickness 0f 0.125" and

bonded to a 2" diameter copper plate using silver epoxy under Ar atmosphere. The Cs_2WO_4 target was found to be very hygroscopic and was stored in vacuum between each operation.

Cs_2WOS_3 target: Cs_2WOS_3 is not available commercially. Dr. James King of Desilube Inc., who has originally developed the material, has provided some powder for fabricating a sputter target. The Cs_2WOS_3 powder was found to decompose on heating above 250°C. No densification was observed below this temperature. In order to fabricate a target with desired strength, about 10 wt% Ag powder was added to Cs_2WOS_3 powder. The powder was then thoroughly mixed using an Agate-mortor and then pressed uniaxially using 10,000 lbs in a 2 inch die. The part was then isostatically pressed at 5,000 psi using Ar gas and was then machined to desired dimension (1.9x0.125"). The target was then bonded in a copper cup using silver epoxy under Ar atmosphere. Again, due to its hygroscopic nature, the target was always stored in vacuum.

WS_2 sputter targets are readily available as an in-stock item with a number of vendors.

3.1.2 Coating Deposition

Deposition of Cs_2WO_4 + WS_2 coating

Coatings were deposited by co-sputtering of Cs_2WO_4 and WS_2 using two sputter guns simultaneously. Cs_2WO_4 was sputtered by using RF power, while WS_2 was sputtered by using DC power. Pure argon at a flow rate of 25 SCCM was used for sputtering. Argon pressure was maintained at about 10 mTorr during the discharge. Polished Si wafers were used as substrates for XPS analysis. Inconel 718 substrates were used for friction tests. The following power settings were employed to generate samples for XPS analysis and friction tests:

Sample	116A	116B	T402	T403
Cs_2WO_4	150 W	150 W	150 W	150 W
WS_2	40 W	30 W	70 W	50 W

A –50 V DC bias was used on the substrate for all coatings. The coating thickness was about 0.5 μm.

Deposition of Cs_2WO_4 and Cs_2WOS_3 Coatings

Coatings of above materials were deposited on Inconel 718 plates using RF sputtering. The substrates were biased to –100V during deposition. Also, bilayer coatings of WS_2 and Cs_2WO_4 were deposited.

3.2 Results of XPS analysis

We have used XPS analysis of two films of Cs_2WO_4 + WS_2 on silicon for the determination of their composition and chemical nature. High-resolution scans of powder standards of these materials were analyzed to aid in these determinations. Figure 1(a) and (b) show the survey scans of samples T402 and T403A, respectively. All the elements that are expected to be present are detected together with carbon as an impurity.

From the powder standard, it was determined that W 4f spectra for WS_2 and for Cs_2WO_4 show $4f_{7/2}$ peaks at 33.2 eV and at 34.9 eV respectively (Figures 2 and 3). The S 2p peak binding energy for WS_2 is 162.8 eV (Figure 4). The S 2p peak binding energy for both samples T402 and T403A is in good agreement with that of the standard. There is no evidence of SO_3 or SO_4 ions which would have peaks in the range from 166 to 170 eV. The W 4f spectra for both films are well-fitted by two $4f_{5/2}$-$4f_{7/2}$ doublets (Figures 5 and 6). The lower binding energy doublet has a $4f_{7/2}$ peak binding energy of 33.2 eV in agreement with that for WS_2. The higher binding energy doublet has a $4f_{7/2}$ peak binding energy of 35.6 eV, which is somewhat higher than that for Cs_2WO_4. This may be due to the presence of some WO_3, which has a $4f_{7/2}$ peak binding energy of 35.9 eV.

Table 1 shows the approximate atomic percent surface compositions of the two films. The measured tungsten levels in the standards are lower than expected from the known stoichiometries. This suggests that there may be an error in the sensitivity factor for the W $4f_{7/2}$ peak. Nevertheless, the results do show that there is proportionately more sulfur and W-S tungsten on sample T402 than on T403B.

The samples T402 and T403B (same run as T403A) were annealed in air at 600°C for 2 hours. The survey XPS scans of these samples are shown in Figures 7(a) and (b). It can be seen that the sulfur peak is absent from both of these scans indicating that sulfur is lost upon annealing. The W 4f scans for both samples show only one $4f_{5/2}$-$4f_{7/2}$ doublet due to WO_4 and /or WO_3. Figure 8 shows the high resolution W 4f scan for the T402 sample. The other W 4f doublet detected previously in the as-deposited sample was for WS_2. Also, the S 2p spectra of these annealed samples show no peak at ~163 eV due to metal sulfide.

From these XPS results it can be concluded that there has been a loss of sulfur due to annealing. The annealed films are composed of Cs_2WO_4 and, possibly, some WO_3.

We have heat treated a sample (T403A) in vacuum (~10^{-6}Torr) at 800°C for about 2 hours. In this case, the substrate was oxidized silicon. Figure 9 shows the survey scans of the sample T403A. All the elements that are expected to be present including sulfur are detected together with carbon as an impurity. The level of sulfur is about the same as that in the as-deposited sample indicating no decomposition of sulfur when heat-treated in vacuum. The S 2p peak binding energy, as shown in the high resolution scan of Figure 10, is similar to that for WS_2. Figure 11 shows the high resolution scans of W 4f spectrum. In fitting the W 4f spectrum for the present sample, it was necessary to use

three $4f_{7/2}$-$4f_{5/2}$ doublets. A comparison of this spectrum with those of WS_2 and Cs_2WO_4, as shown in the previous report, reveals that peaks 1 and 2 are due to WS_2, and peaks 3 and 4 are due to Cs_2WO_4. These four peaks also correspond to similar peaks on the as-deposited films. Additionally, in the present film, there is a higher binding energy component (peaks 5 and 6) that has not been observed previously. In order to determine whether these extra peaks correspond to Cs_2WOS_3, we have analyzed the powder sample of this material obtained from Dr. James King.

The sample for XPS analysis was prepared by distributing some of the powder on adhesive tape. The survey scan of the Cs_2WOS_3 powder is shown in Figure 12. In addition to the expected elements, Na is detected as impurity in the sample. Also, there is more oxygen and less sulfur than would be predicted from the expected stoichiometry of this powder. The high-resolution scan of W 4f peak is shown in Figure 13. The W 4f spectrum could be fitted with two $4f_{7/2}$-$4f_{5/2}$ doublets. The higher energy doublet (peaks 3 and 4) correspond to the unknown higher binding energy component that was observed in the vacuum heat-treated film (Figure 11). The other W 4f doublet (peaks 1 and 2) are probably due to some Cs_2WO_4 on the surface of the powder.

From these XPS results it can be concluded that there has been a solid phase reaction between WS_2 and Cs_2WO_4, and the reaction products include Cs_2WOS_3.

3.3 Friction Tests

Friction tests were performed at the Cleveland State University under the supervision of Dr. Earl Graham. Figure 14 shows the pin-on-plate wear tester used for these tests. It consists of a cabinet fitted with top plate (2), which is reciprocated using a variable speed drive system. The plates, 12 cm x 0.5 cm and 0.3 cm thick, were attached inside the cabinet. The required load was applied on the pin (1) by hanging the weights at the end of the horizontal bar (5) of the force post holding the pin. The pins had a flat end and were 2.6 cm long and 0.63 cm in diameter with a 45° tapered tip. The diameter of the tapered pins at the flat end was 0.25 cm. The contact area of the pins was 0.049 cm^2. The reciprocating motion of the plate resulted in the pin rubbing against the surface of the plate. An average linear velocity of 12.7 cm s^{-1} (corresponding to 90 rpm) over a 4 cm long wear track was used. One transducer (3) measured the friction force and the other (7) the pin and plate wear, in terms of the wear depth. This method of measuring wear accounts for both wear of the pin and plate. Separate studies were made in which the weight loss of both the pin and plate were measured. The results from these studies correlated very well with the wear as recorded by the transducer. The transducers were insulated from the metal holders with high temperature tape to insure stable operation when the plate was heated. The transducers were connected to a data acquisition unit which was capable of taking 100 data samples per second. Because of the reciprocating motion, the plate and the pin came to rest at the end of each cycle. The rod impacting on the friction force transducer vibrated vigorously towards the end of the cycles, resulting in erratic data. Therefore, a triggering arrangement was used to prevent the data acquisition near the end of the cycle. Data was inquired only when pin was sliding. The specimen was heated by resistance heating.

As mentioned earlier, coatings were deposited on Inconel 718 plates for the friction tests. Pins were made of cast iron. A load of 1.5 kg was used for these tests in air. Figures 15(a),(b) and (c) show the friction traces for the sample 168-0116A at room temperature (RT), 400°C and 600°C, respectively. The coefficient of friction at RT was about 0.2 for the first 7 minutes and then increased to about 0.5 afterwards. At 400°C, the coefficient of friction started at about 0.4 and then gradually reduced to about 0.2 after about 10 minutes. At 600°C, the coefficient of friction ranged between 0.3 and 0.4 for most of the time except the very beginning when it was somewhat higher.

Figures 16(a), (b) and (c) show the coefficient of friction for the sample 168-0116B at RT, 400°C and 600°C, respectively. The coefficient of friction at RT was lower than 0.2 for this sample; however, at 400°C it was higher, ~0.4. At 600°C, the coefficient of friction was lower, ~0.3, than that at 400°C.

Pure WS_2 films show a friction coefficient ~0.1-0.15 in air at temperatures below 460°C (Figure 17). The friction coefficient of Cs_2WO_4 is not available in the literature. In order to properly interpret the data on friction coefficient of $WS_2 + Cs_2WO_4$ at various temperatures, it is necessary to know the friction coefficient of Cs_2WO_4 in that temperature range. Therefore, Cs_2WO_4 coatings were deposited on Inconel 718 substrates for friction measurements. In addition, we have produced two multilayer films of Cs_2WO_4 and $Cs_2WO_4 + WS_2$ for friction measurements. Since sulfur escapes from WS_2 in a $Cs_2WO_4 + WS_2$ film when the film is heated in air at temperatures above 450°C, a multilayer of the mixed film and Cs_2WO_4 may prevent a rapid loss of sulfur thus forcing the reaction to form Cs_2WOS_3 phase. The layer structure of these films is shown schematically in Figure 18. The total thickness of these films was about 1 μm. The thickness of the individual layers was not measured.

Friction coefficients of films shown schematically in Figure 18 and a single layer of Cs_2WO_4 , all on Inconel 718 substrates were measured at temperatures in the range room temperature to 550°C in room air.

Figures 19a,b,c show the friction coefficient as a function of time for the sample 168-0419A at room temperature, 300°C and 550°C, respectively. Friction coefficients are less than 0.1 at room temperature and at 550°C, but slightly higher than 0.1 at 300°C. The details of the friction trace such as sudden steep rise of the friction coefficient and subsequent fall within the test duration (Figure 19c) are not clear at this time. Figures 20a,b,c show the traces of friction coefficient as a function of time for the sample 168-0419B at room temperature, 300°C and 550°C, respectively. In this case, the friction coefficient at 550°C is higher, ~0.2, as compared to that of the sample 168-0419A. The friction coefficients at lower temperatures are comparable to that of the other sample. More detail analysis is required to elucidate the features observed in the friction traces.

Figures 21a,b,c show the friction coefficient as a function of time for the single layer Cs_2WO_4 at room temperature, 300°C and 530°C, respectively. The friction traces at

room temperature and 300°C are quite smooth and the friction coefficient is low, ~0.1-0.13. At 530°C, the friction coefficient started higher, ~0.3, and then slowly decreased to about 0.13 after 5 minutes. It appears that the friction coefficient may not have reached a steady state. Further investigations of this new material as a solid lubricant is worthwhile.

Figures 22a,b show the friction coefficient as a function of time for the single layer Cs_2WOS_3 at 300°C and 530°C, respectively. The friction coefficient is about 0.3 at 300°C and about 0.25 at 530°C.

4.0 SUMMARY AND CONCLUSION

The purpose of the present work was to develop a solid lubricant coating that can function over a broad temperature range. The proposed approach was to develop adaptive lubricant coatings from materials that undergo chemical change with increasing temperature by reacting together and with the environment. Specifically, in Phase I, we have studied the feasibility of formation of high temperature lubricant material cesium oxythiotungstate (Cs_2WOS_3) on Inconel 718 surface from a composite coating of cesium tungstate (Cs_2WO_4) and tungsten sulfide (WS_2) upon exposure at high temperature in air. The hope was that WS_2 would provide low friction up to about 400°C and then react with Cs_2WO_4 to form Cs_2WOS_3 that can provide lubrication up to about 600°C. The results obtained in Phase I clearly indicate that sulfur escaped from the composite coating upon exposure to temperature above 500°C in air instead of forming the desired higher temperature lubricating compound. However, exposure at higher temperature in vacuum resulted in the formation of the desired phase. Therefore, an adaptive lubricant could not be formed in laboratory air atmosphere as desired thus limiting the potential use of this research. However, there may still be some limited applications such as in space where the applications of MoS_2 and WS_2 are quite prevalent. A composite of one of these sulfides with Cs_2WO_4 will promote the formation of cesium oxythiotungstate or molybdate at elevated temperature in space environment.

One interesting result of this research is that Cs_2WO_4 coating demonstrated low friction up to 530°C similar to that of Cs_2WOS_3. This indicates that the low friction of Cs_2WOS_3 at high temperatures may be due to Cs_2WO_4 that may have formed as a result of decomposition. Further detailed analysis is needed to determine the usefulness of Cs_2WO_4 as a lubricant for applications over a wide temperature range.

In conclusion, the feasibility of formation of an adaptive high temperature lubricant could not be demonstrated in Phase I in air ambient. However, the desired lubricant phase, Cs_2WOS_3, formed from a composite of WS_2 and Cs_2WO_4 in vacuum environment.

5.0 POTENTIAL APPLICATIONS

High temperature lubricant coatings can be used in metal and ceramic bearings for high temperature applications. Ceramics are being considered for gas turbine engine

applications such as in seals and bearings, variable stator vanes, etc. Gas turbine engines can run at higher temperature and therefore more efficiently if suitable high temperature lubricants are available. The interest in this technology is widespread among all branches of government and industry: Air Force, Army, Navy, NASA, BMDO; and engine manufacturers General Electric, Pratt & Whitney, Allison, Garrett, Teledyne, Textron Lycoming, and Williams.

Solid lubricant coatings are extensively used in spacecraft. Launch vehicles and spacecraft have various release mechanisms that permit the spacecraft to separate from the launch vehicle. Spacecraft also have deployment mechanisms that allow subsystems (e.g., antenna dishes, solar panels), which are often folded during launch to conserve volume, to be opened in orbit. These release or deployment mechanisms require a lubricant to provide low friction (torque) for a low number of cycles. Lack of thermal control may require the lubricant to function in a wide temperature range.

Besides the turbine engine and space applications, advanced high temperature lubricants and systems are needed in the industries such as automotive, metal-cutting/forming, high-vacuum equipment, and industrial machinery.

REFERENCES

1. J. K. Lancaster, "CRC Handbook of Lubricants," Vol II, p. 269.
2. H. E. Sliney, Symposium on Lubricants for Extreme Environments at the ASME/ASLE Lubrication Conference, Washington, DC, October 5-7, 1982, p. 1.
3. H. E. Sliney, NASA TM D-5301, 1969.
4. J. P. King and N. H. Forster, "Synthesis and Evaluation of Novel High Temperature Solid Lubricants," AIAA Paper 90-2044 (1990).
5. A. K. Rai and R. S. Bhattacharya, J. Mat. Res. 6 (1991) 2375.
6. J. S. Zabinski, M. S. Donley, V. J. Dyhouse, and N. T. McDevitt, "Chemical and Tribological Characterization of PbO-MoS_2 Films Grown by Pulsed Laser Deposition", Thin Solid Films, 214 (1992) 156-163.
7. M. B. Peterson, S. Z. Li, and S. F. Murray, "Wear Resistant Oxide Films for 900°C", Final Report, Argonne National Laboratory, Subcontract No. 20082401, ANL/OTM/CR-5 (1994).
8. R. F. Bunshah et al., "Deposition Technologies for Films and Coatings: Developments and Applications," Noyes Publications (1982).
9. R. S. Bhattacharya, A. K. Rai and C. S. Yust, "Ion Beam Processing of High-Temperature Solid-Lubricating Coatings", Lub. Eng. 49 (1993) 563.
10. R. S. Bhattacharya, A. K. Rai, and A. Erdemir, "High Energy (MeV) Ion Beam Modification of Sputtered MoS_2 Coatings on Sapphire" Nucl. Instr. Meth. in Phys. Res. B59/60, (1991) 788.
11. R. S. Bhattacharya, A. K. Rai and V. Aronov, Tribology Transactions, Vol 34, (1991) 472.
12. R. S. Bhattacharya, A. K. Rai, A. W. McCormick, A. Erdemir, "High Energy (MeV) Ion Beam Modifications of Sputtered MoS_2 Coatings on ceramics," Tribology Transactions Vol 36 (1993) 621-626.

Table 1

Approximate Atom % Surface Compositions of Cs_2WO_4 / WS_2 thin films and standards, as determined by XPS

Sample	C	O		Cs	S	W	
		O-C, -OH,	O-W, O-S,		S-W	W-O	W-S
T402	42.3	6.7	28.1	1.9	11.9	6.1	3.1
T403A	42.0	9.4	26.4	2.3	9.5	7.5	2.9
WS_2	54.7	12.1	---	---	23.6	---	9.6
Cs_2WO_4	59.6	---	24.9	12.0	---	3.5	---

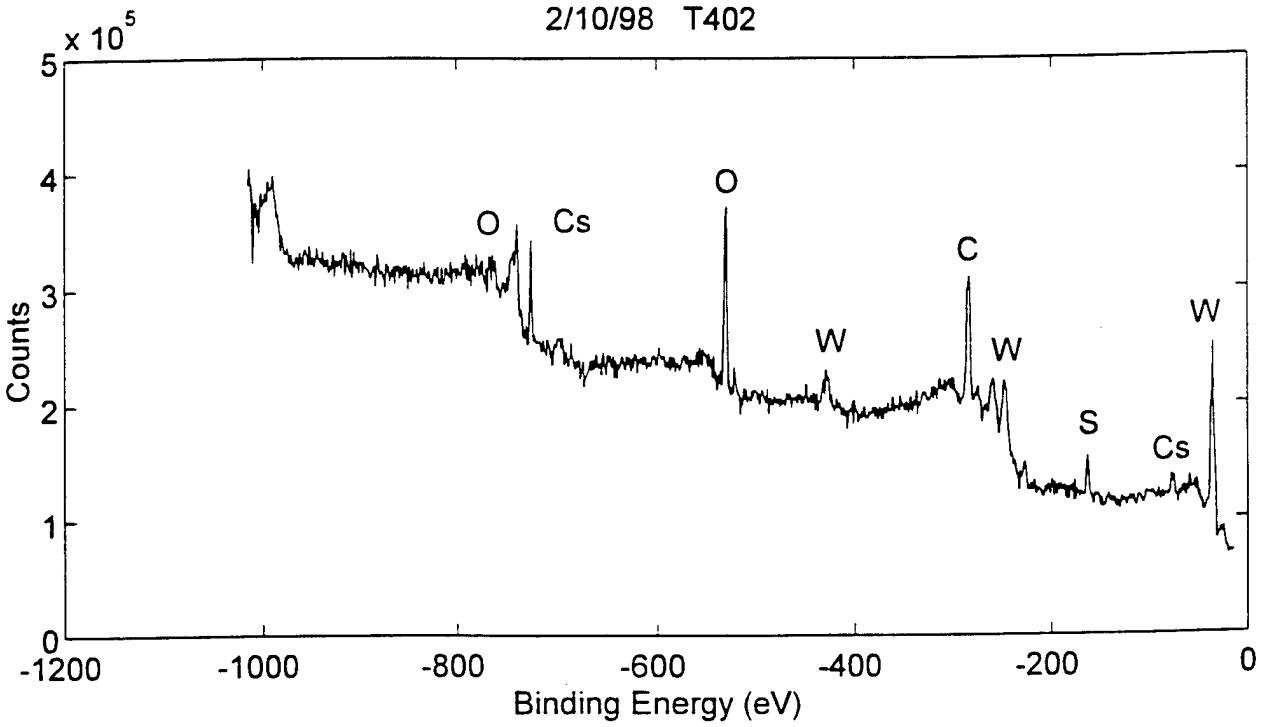

Figure 1a Survey XPS scan of sample T402.

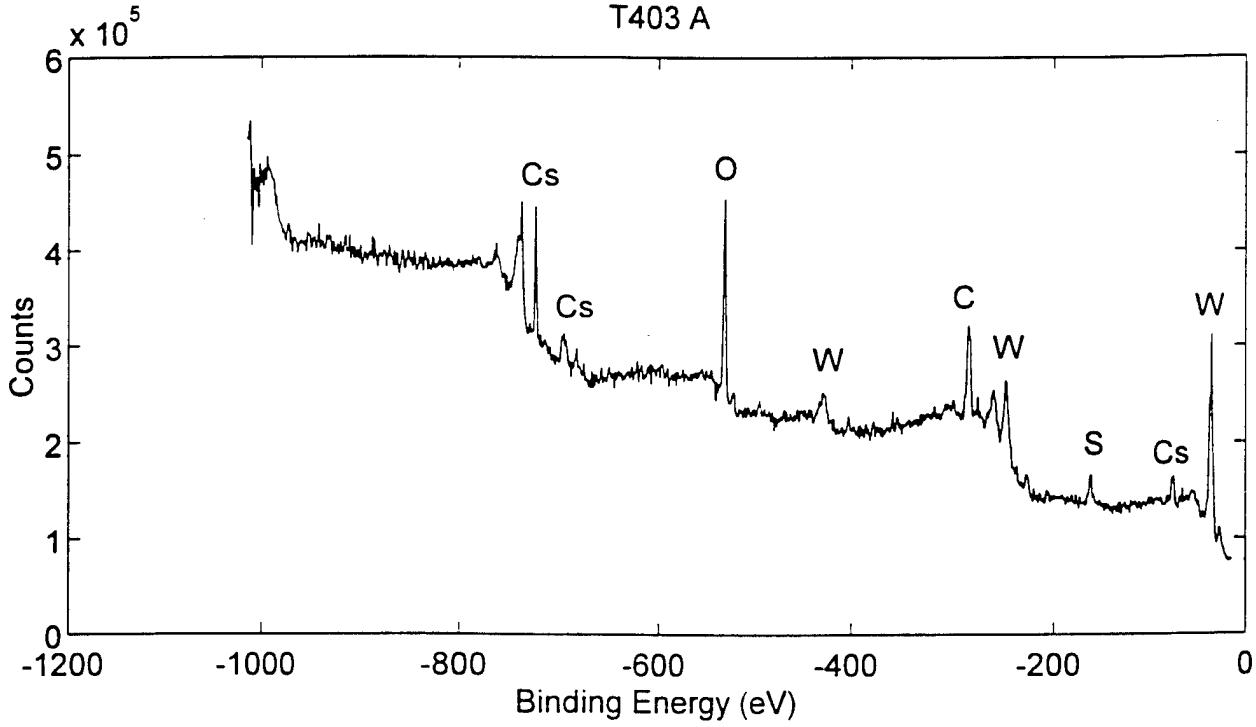

Figure 1b Survey XPS scan of sample T403A.

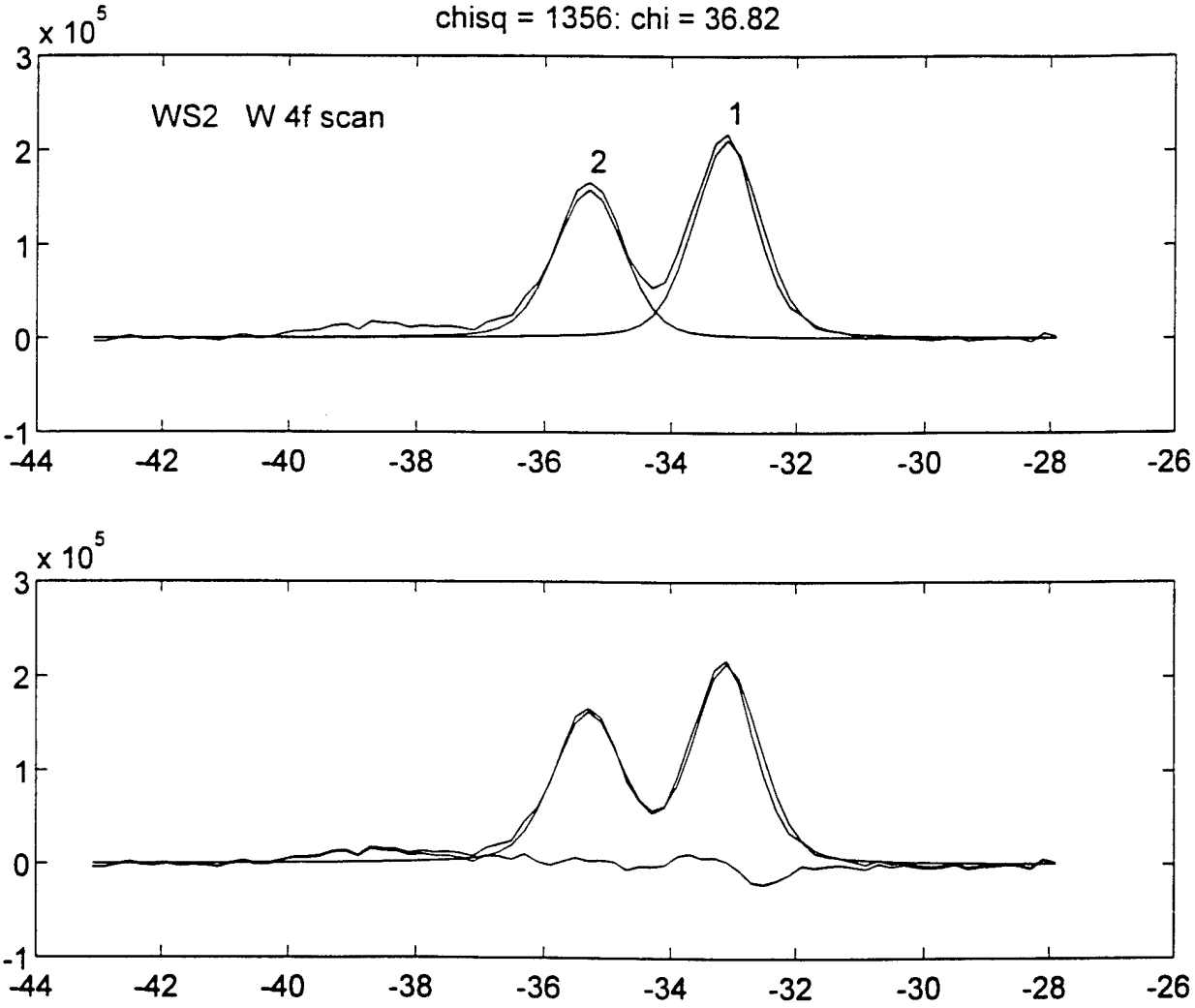

Figure 2 High resolution XPS scan of W 4f peaks from WS_2 powder standard.

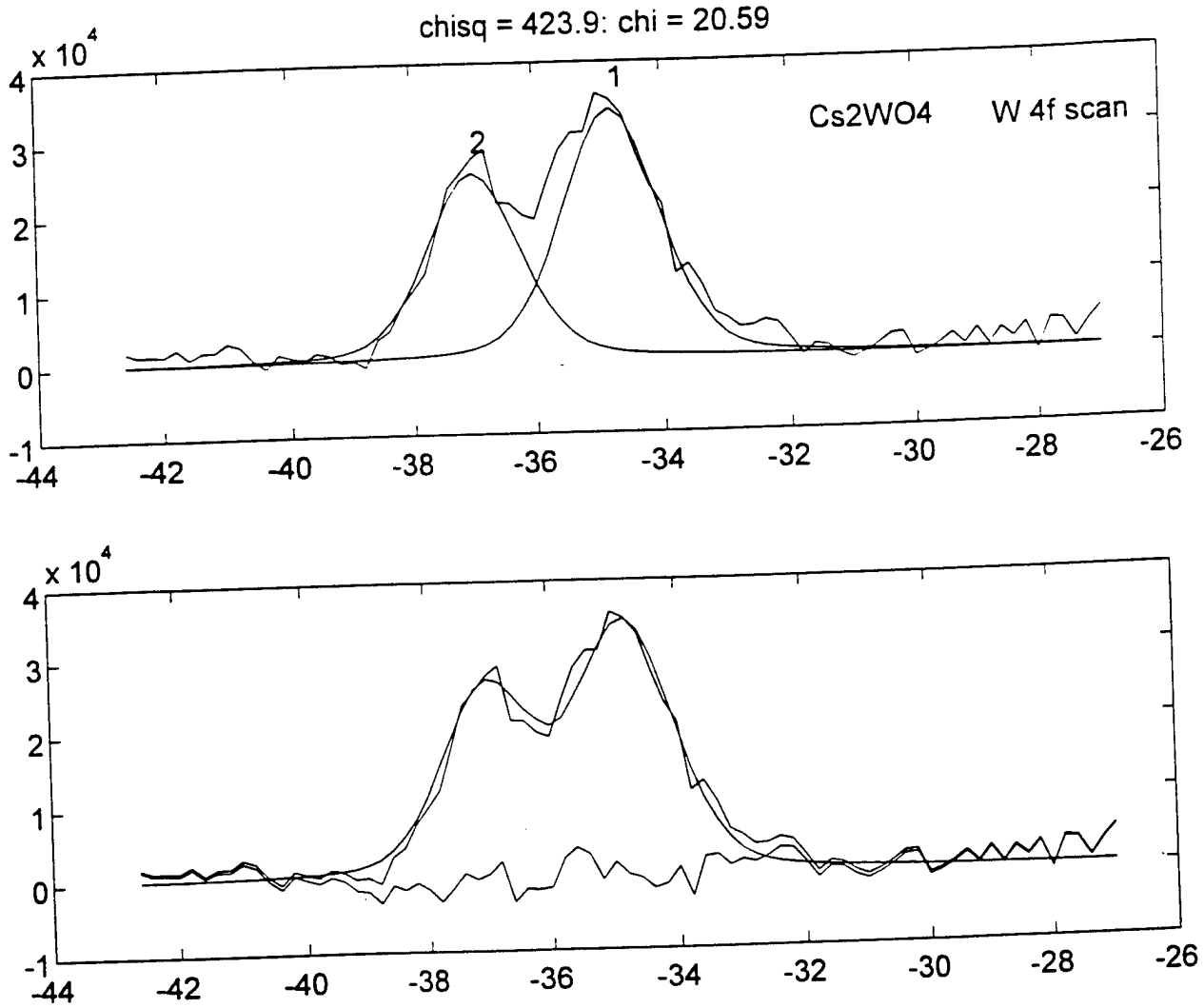

Figure 3 High resolution XPS scan of W 4f peaks from Cs_2WO_4 powder standard.

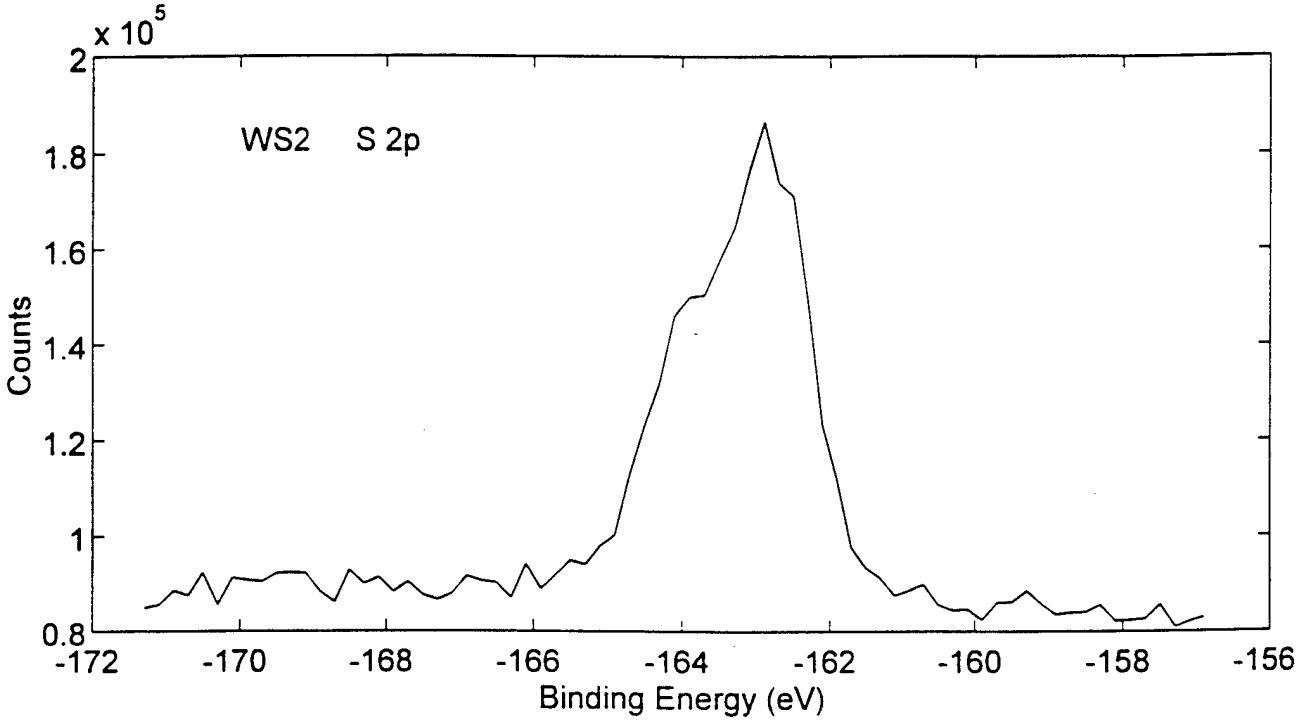

Figure 4 High resolution XPS scan of S 2p peak from WS_2 powder standard.

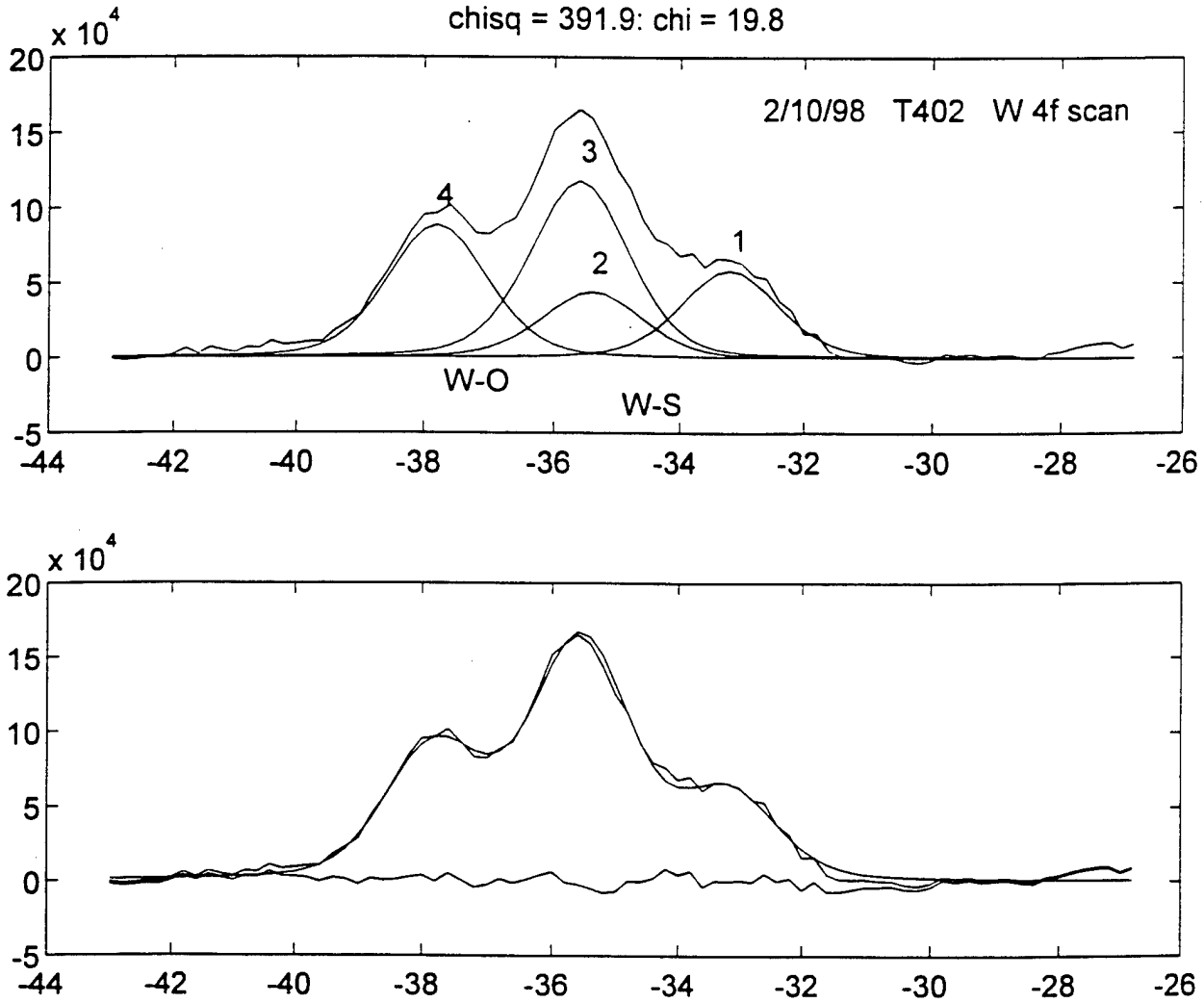

Figure 5 High resolution XPS scan of W 4f peaks from sample T402.

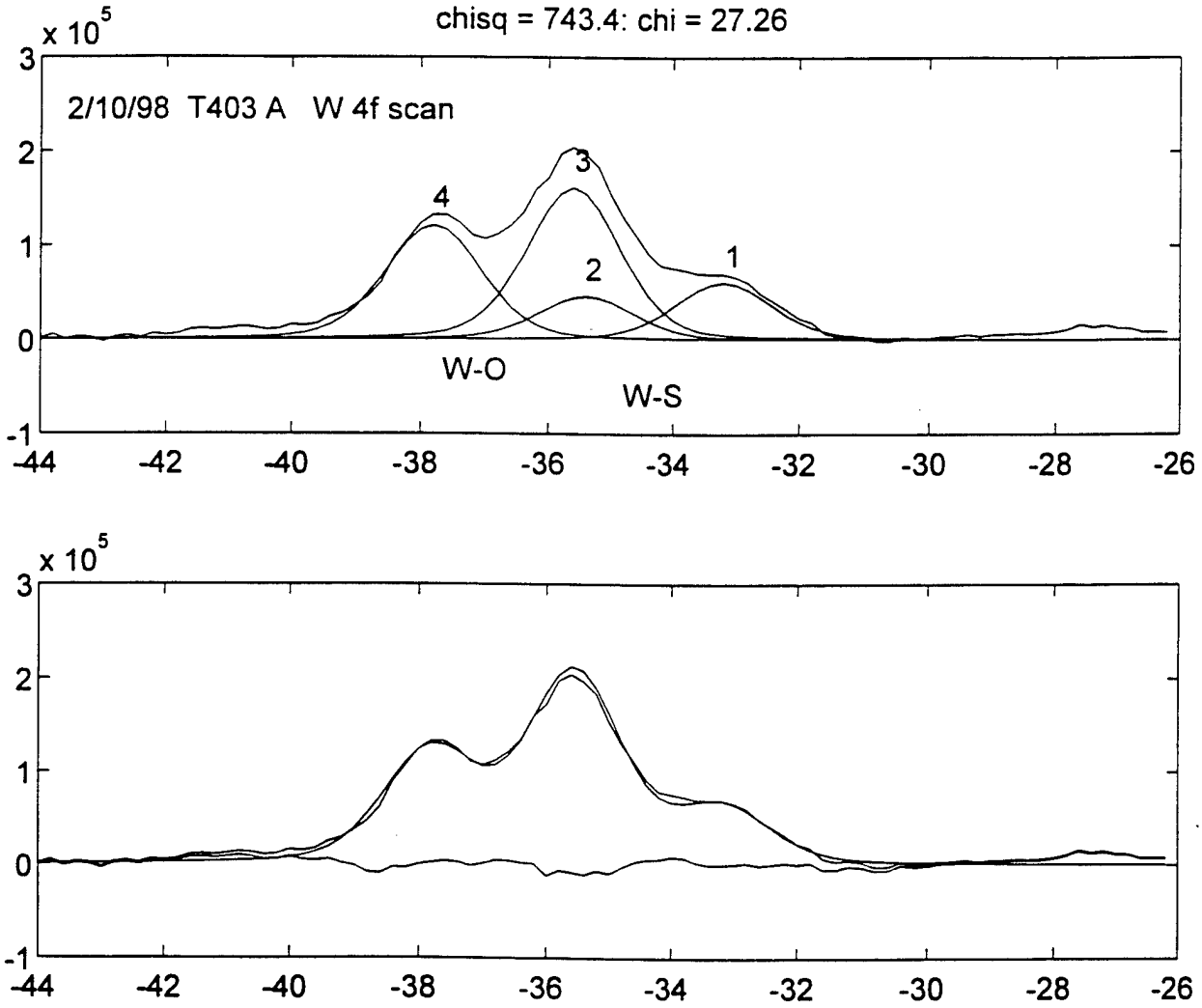

Figure 6 High resolution XPS scan of W 4f peaks from sample T403A.

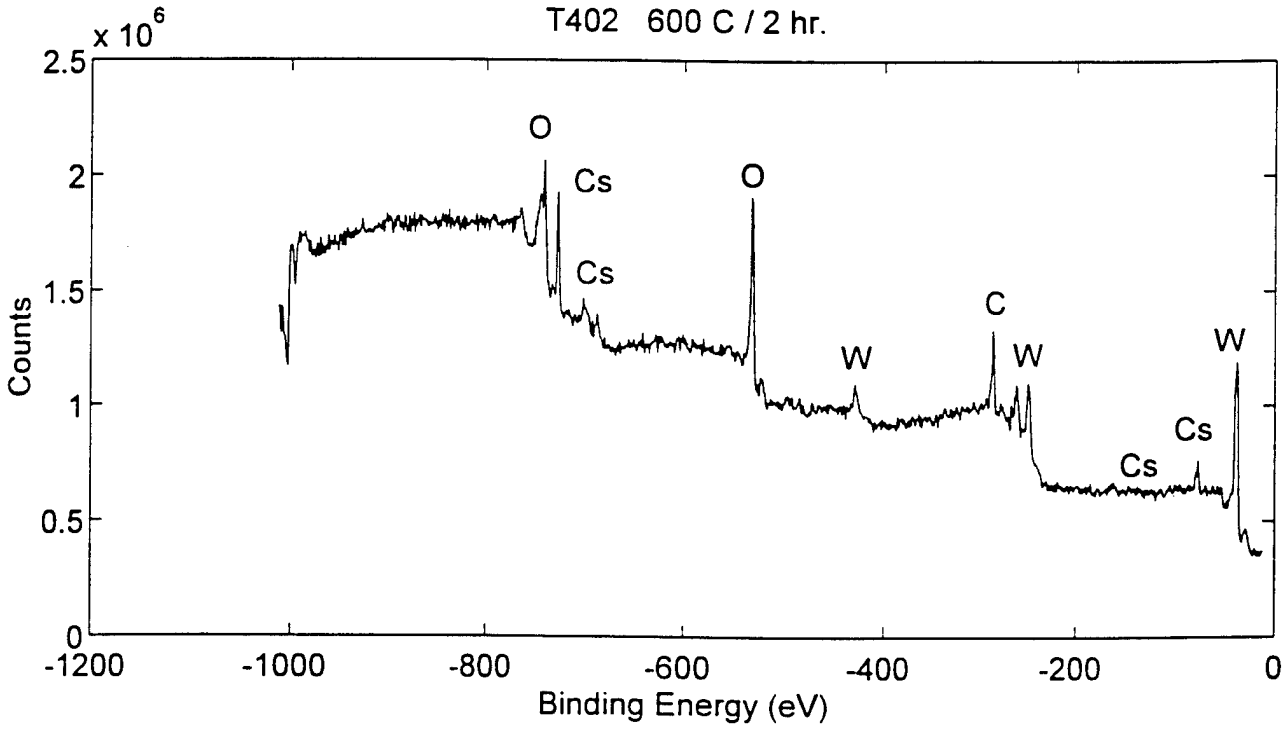

Figure 7a Survey XPS scan of sample T402 after heat treatment at 600°C for 2 hours.

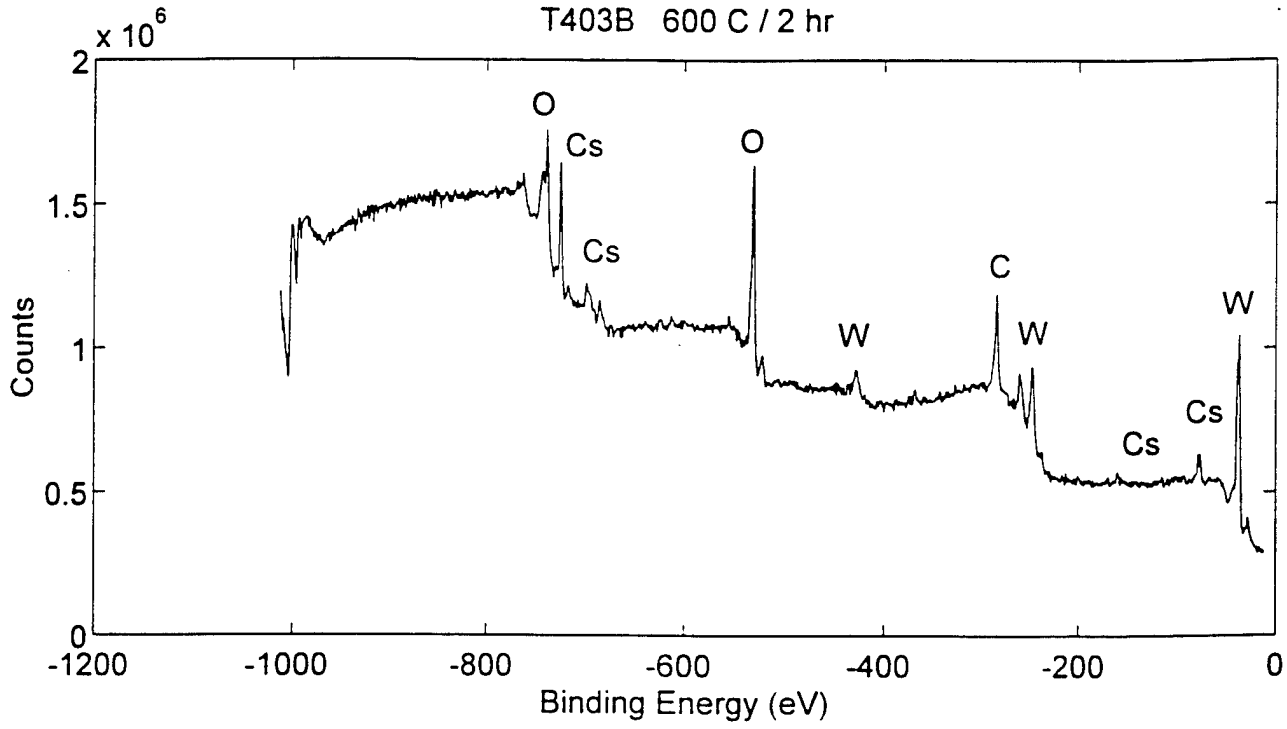

Figure 7b Survey XPS scan of sample T403B after heat treatment at 600°C for 2 hours

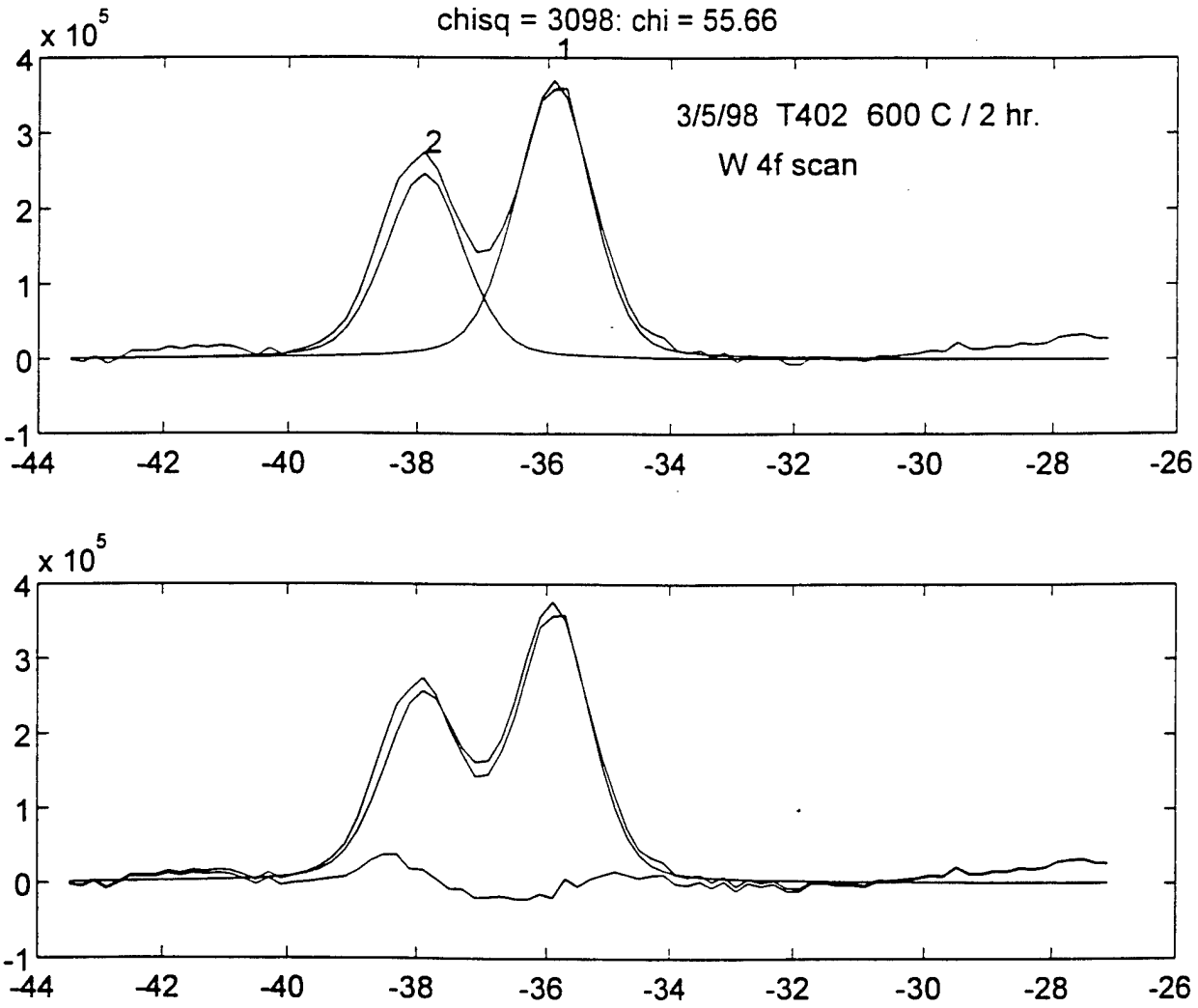

Figure 8 High resolution XPS scan of W 4f peaks from sample T402 after heat treatment at 600°C for 2 hours.

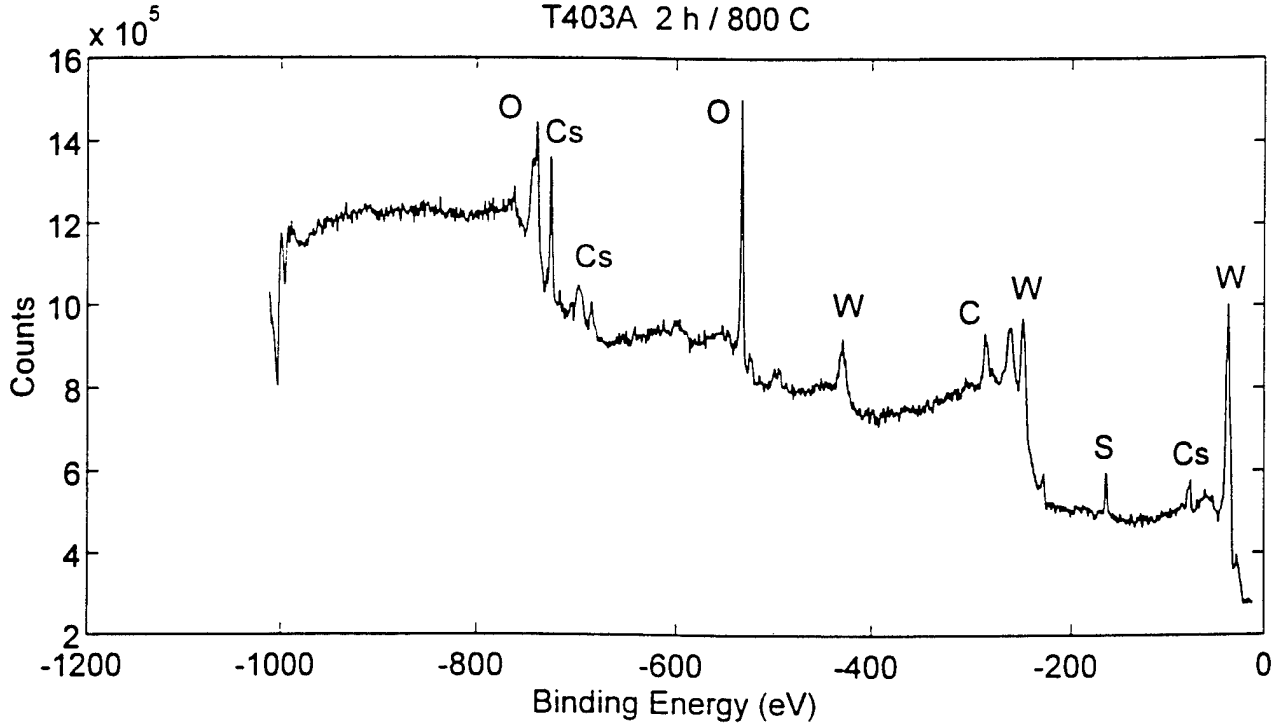

Figure 9 Survey XPS scan of vacuum annealed (800°C) film of WS_2 + Cs_2WO_4.

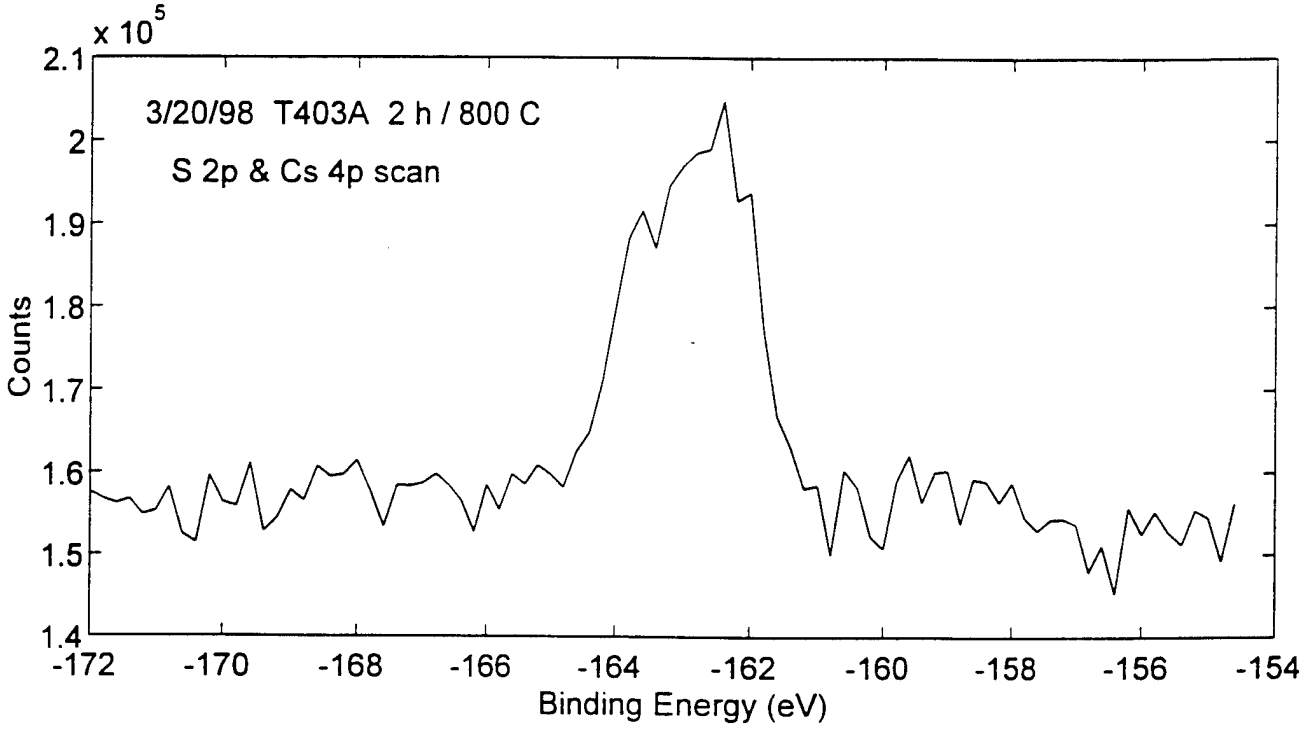

Figure 10 High resolution XPS scan of S 2p peak from the vacuum annealed $WS_2 + Cs_2WO_4$ film.

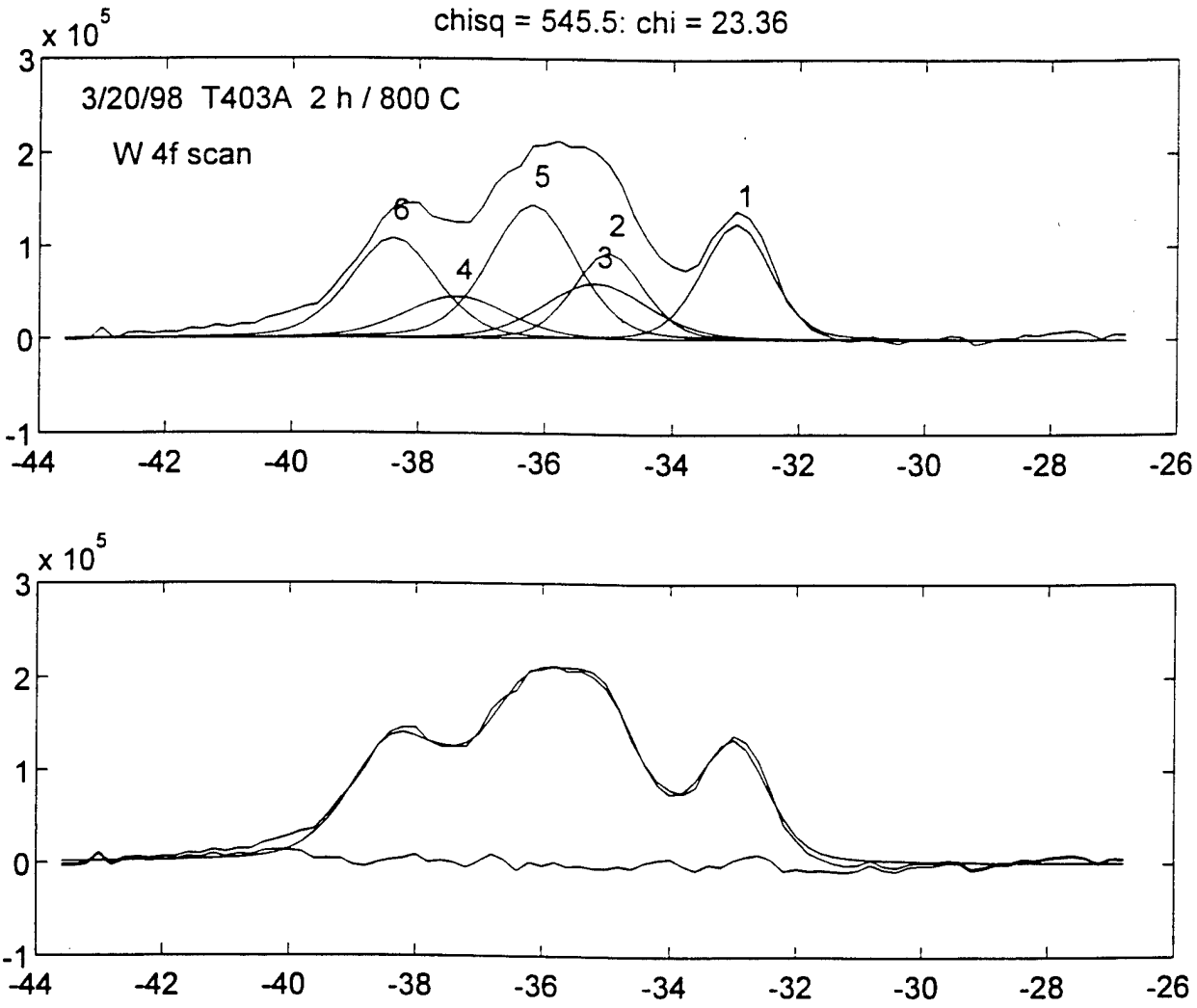

Figure 11 High resolution XPS scan of W 4f peaks from annealed WS_2 + Cs_2WO_4 film.

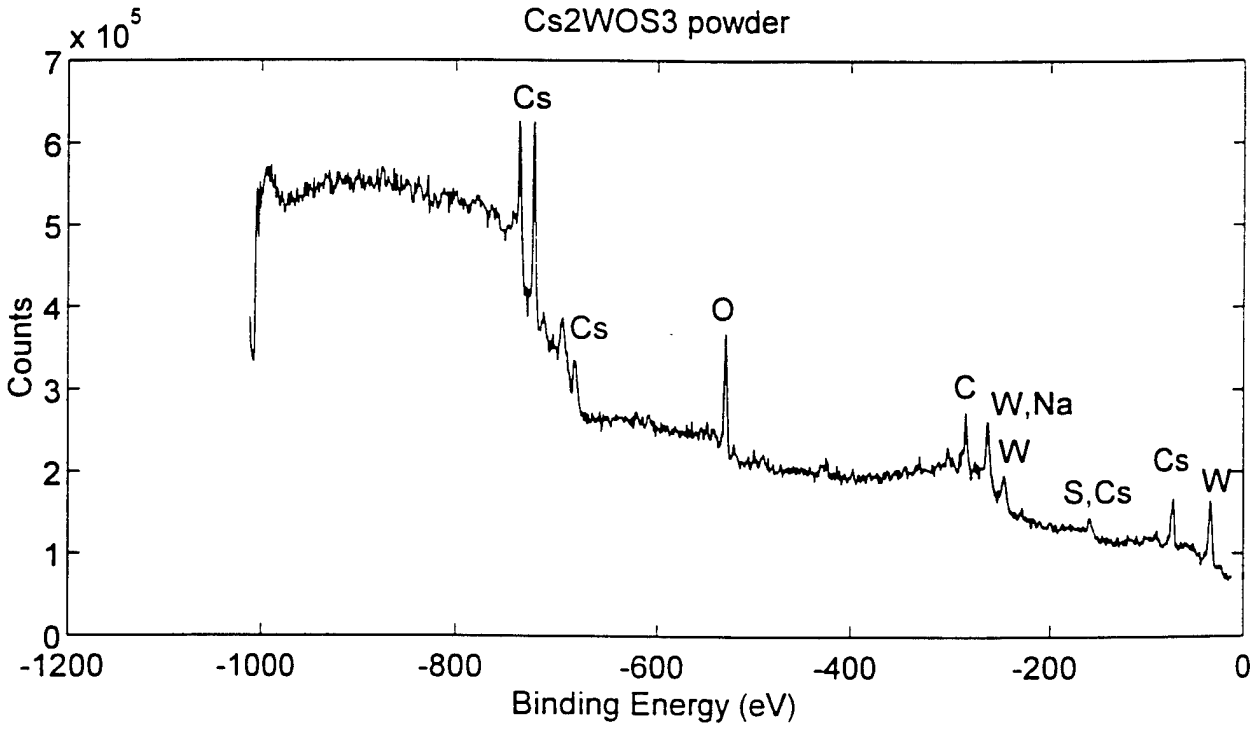

Figure 12 Survey XPS scan of powder sample of Cs_2WOS_3.

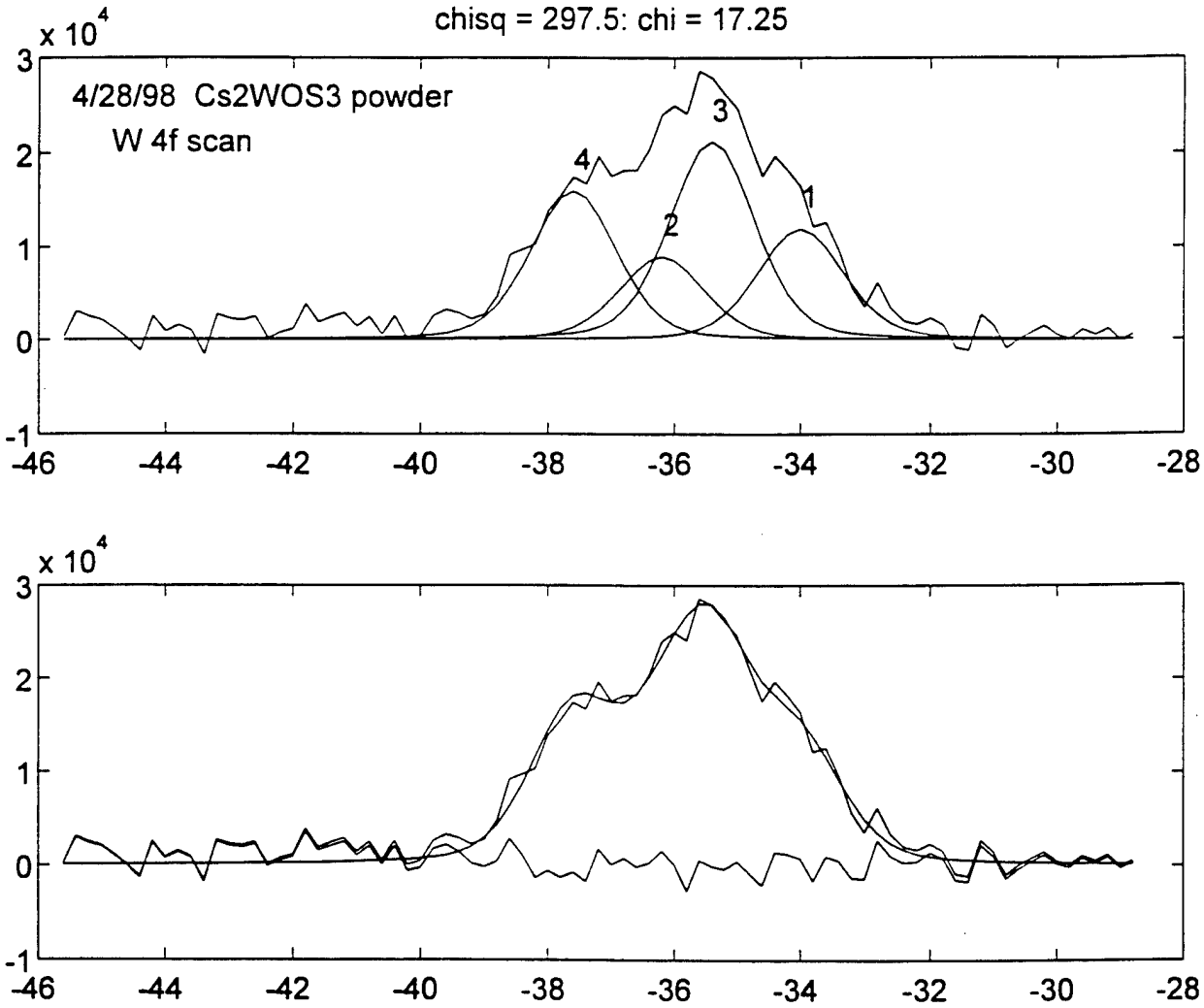

Figure 13 High resolution XPS scan of W 4f peaks from Cs_2WOS_3.

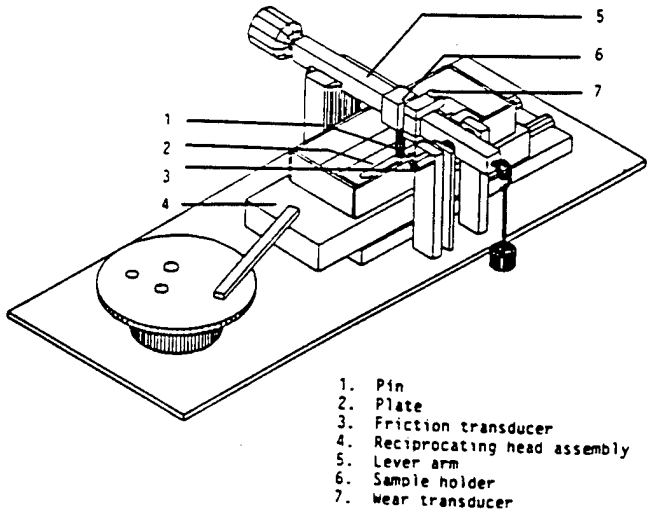

Figure 14 Schematic diagram of the pin-on-plate friction and wear tester at the Cleveland State University.

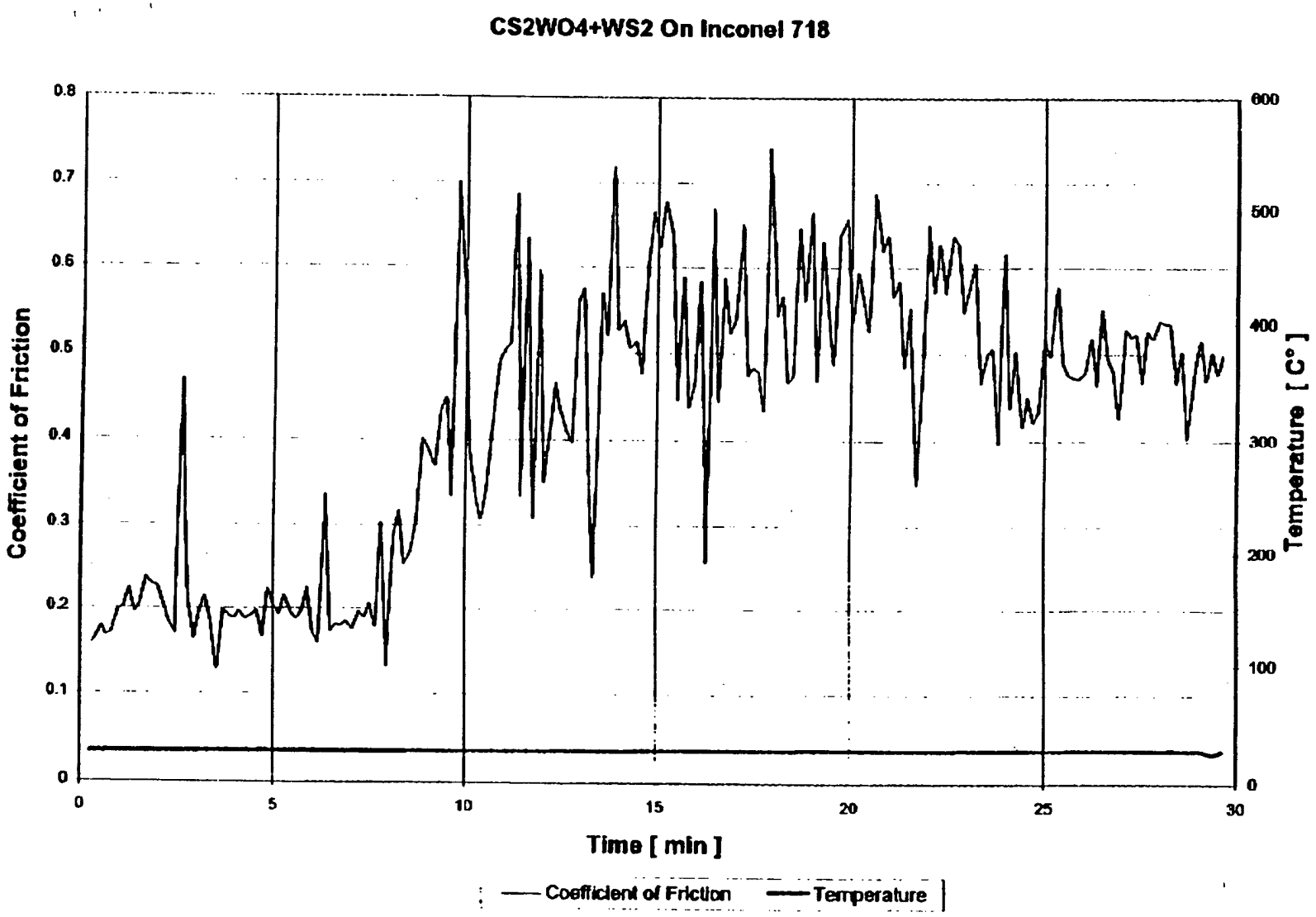

Figure 15a Plot of friction coefficient as a function of time of sample 168-0116A at room temperature.

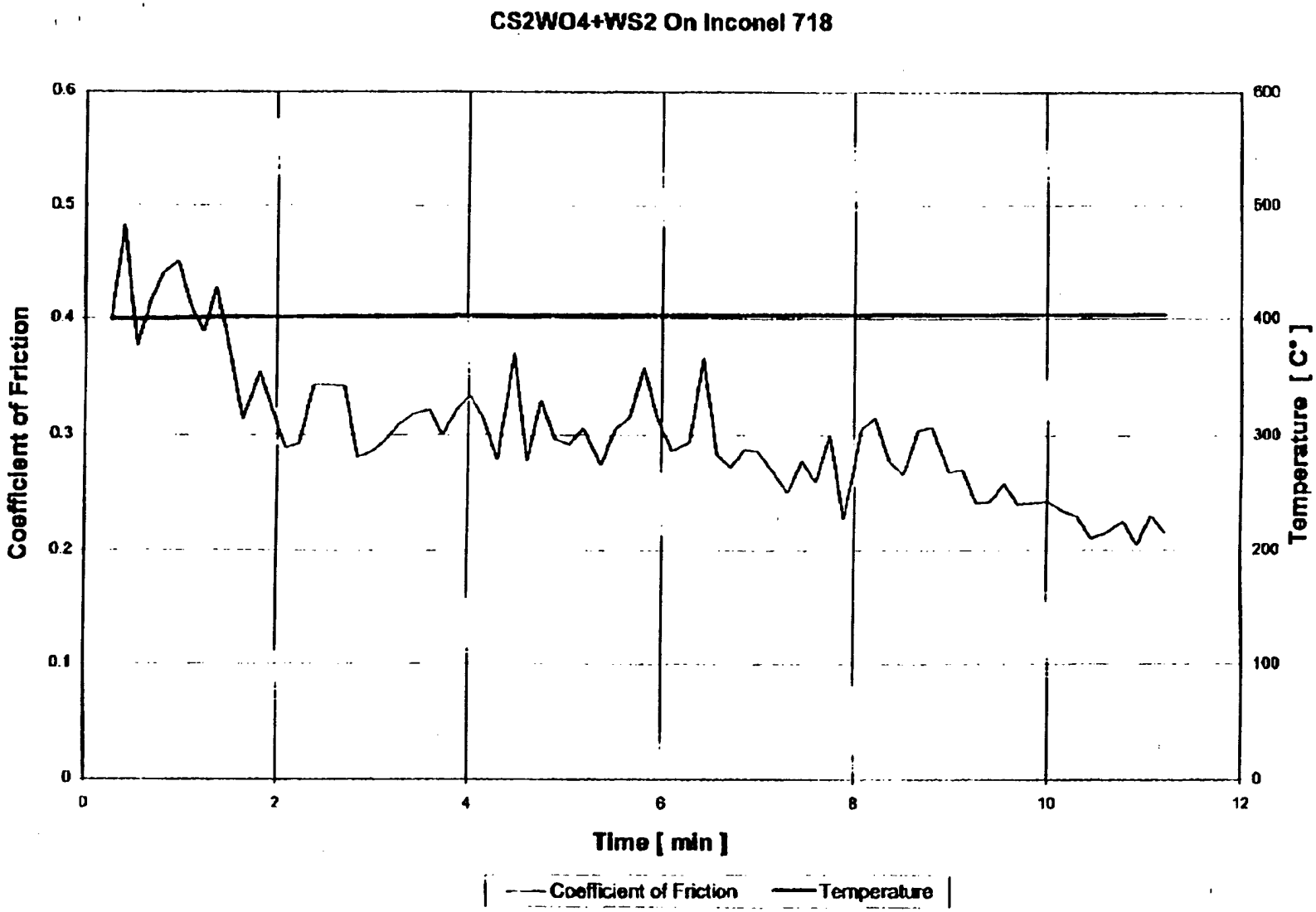

Figure 15b Plot of friction coefficient as a function of time of sample 168-0116A at 400°C.

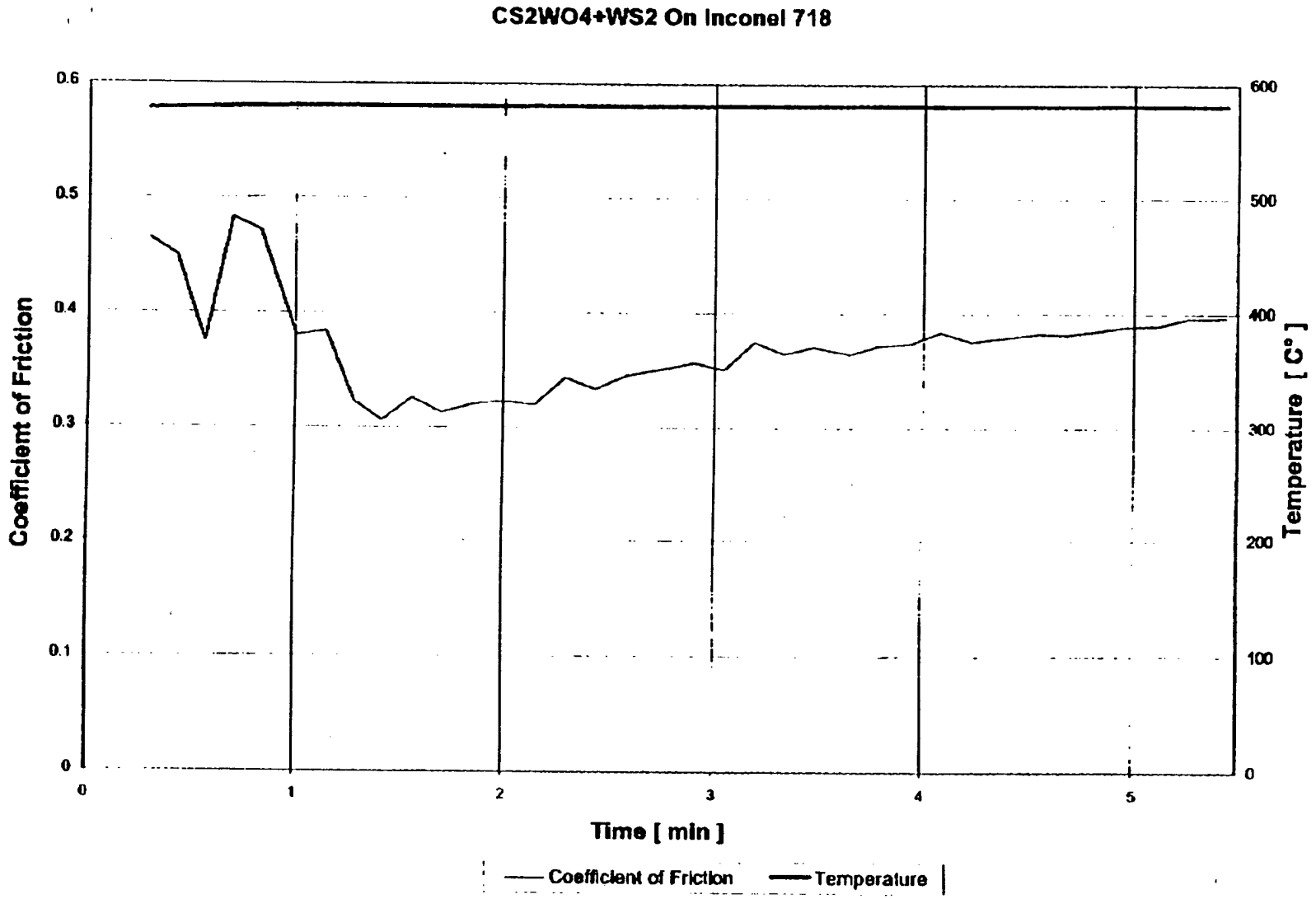

Figure 15c Plot of friction coefficient as a function of time of sample 168-0116A at 600°C.

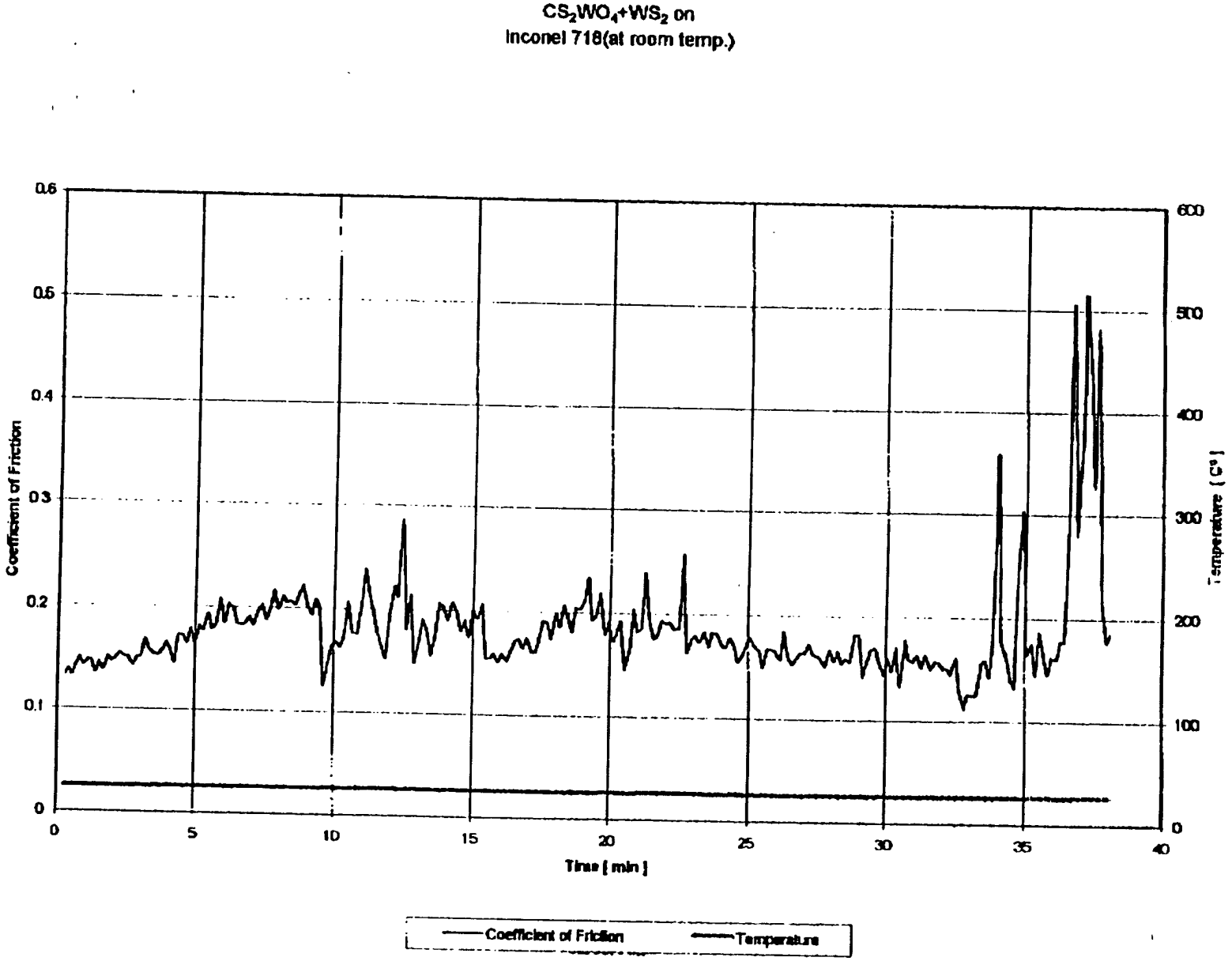

Figure 16a Plot of friction coefficient as a function of time of sample 168-0116B at room temperature

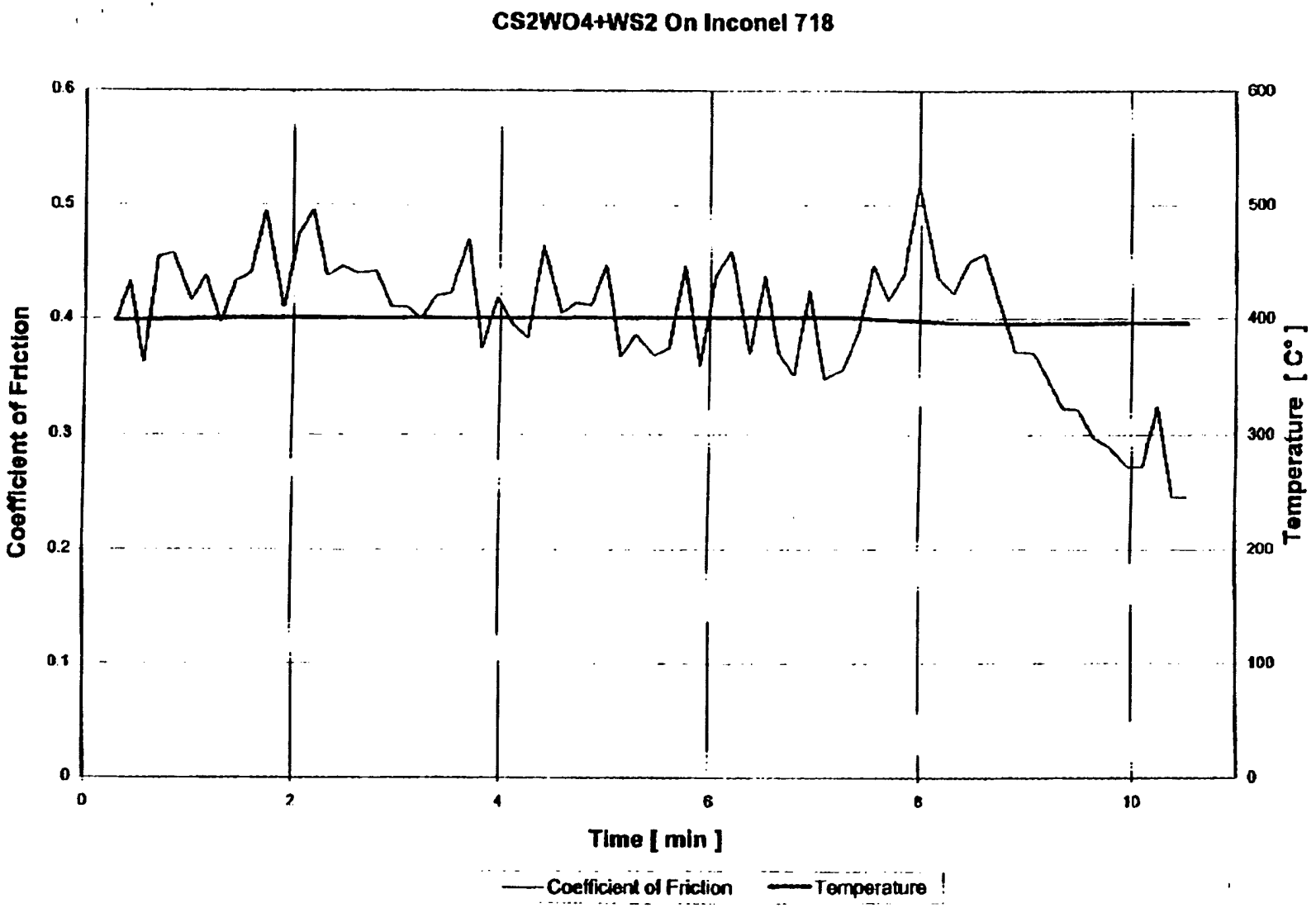

Figure 16b Plot of friction coefficient as a function of time of sample 168-0116B at 400°C.

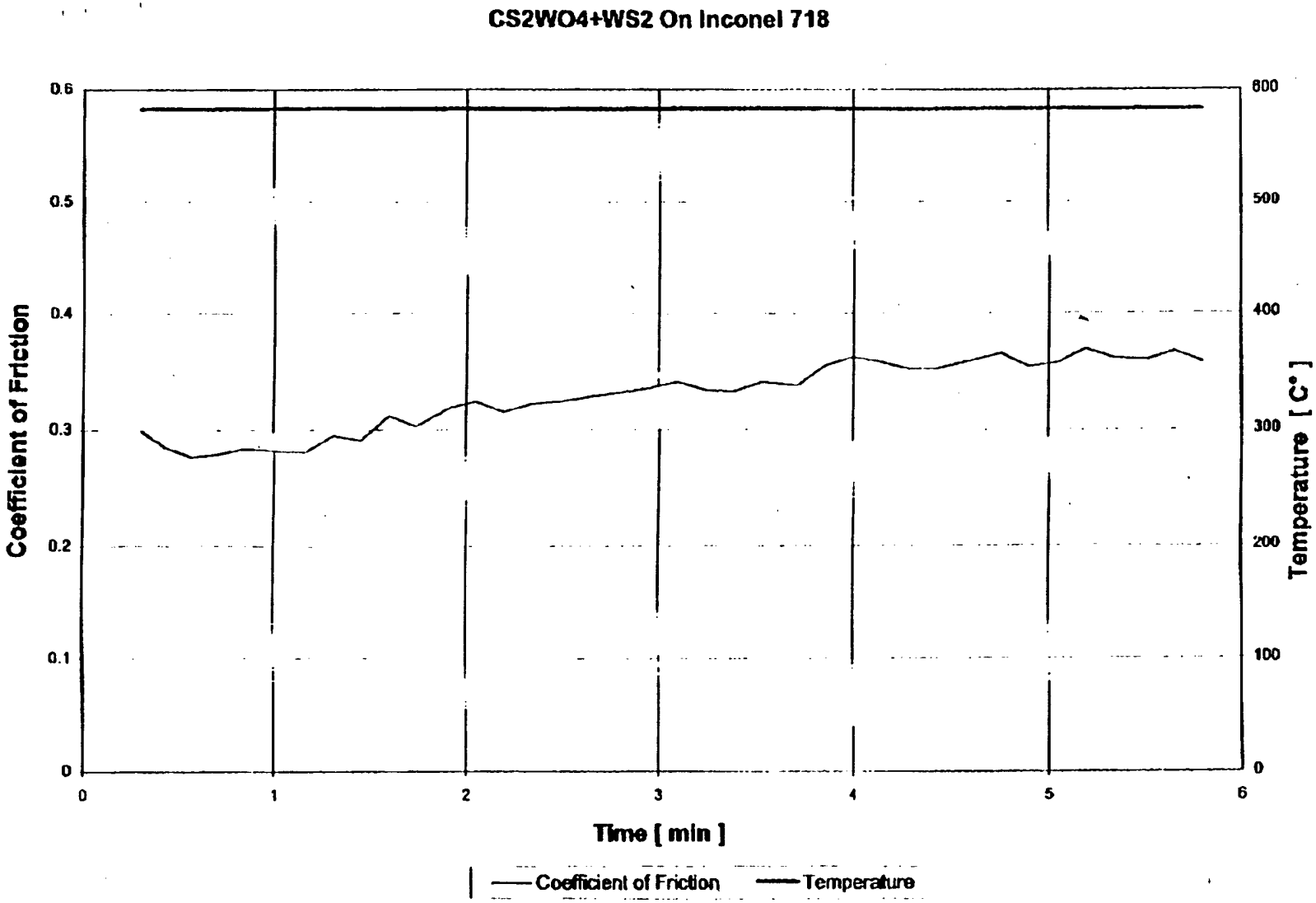

Figure 16c Plot of friction coefficient as a function of time of sample 168-0116B at 600°C

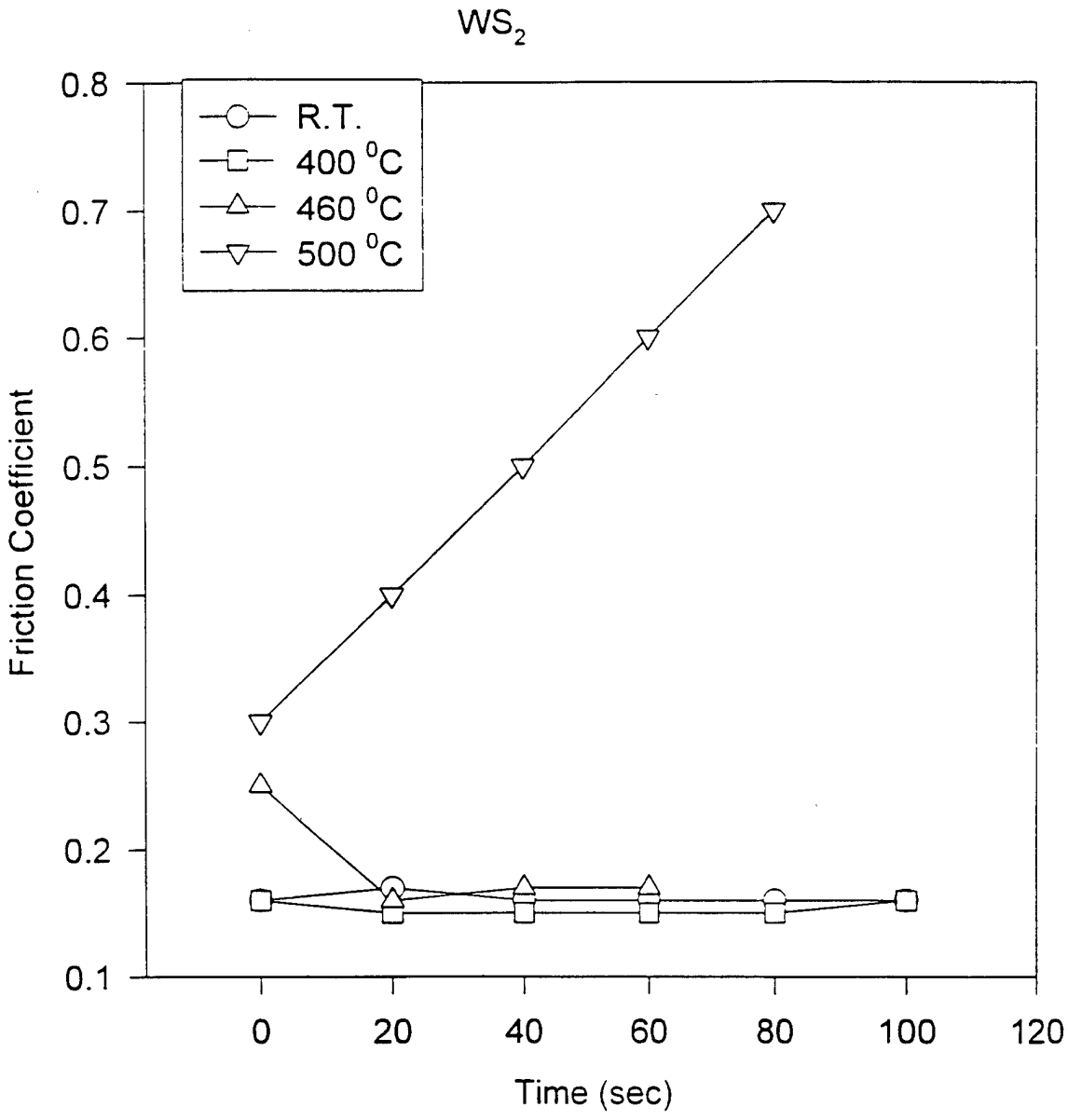

Figure 17 Friction coefficient of WS_2 film at various temperatures.

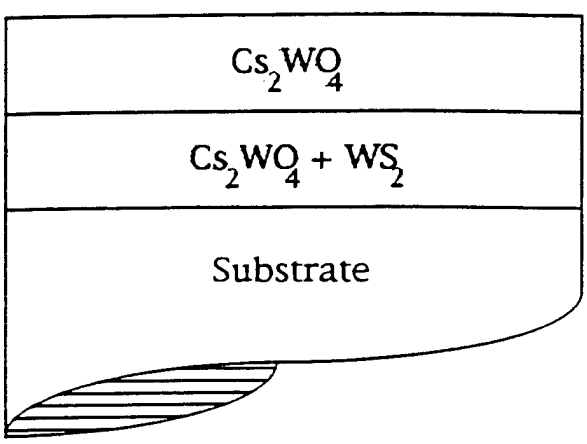

168-0419 A

a

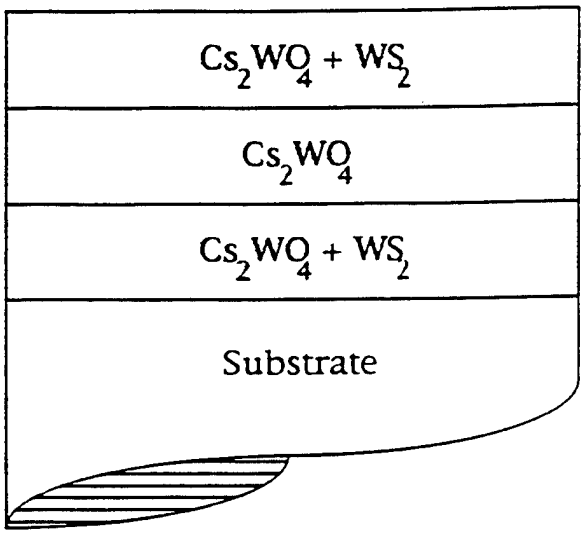

168-0419 B

b

Figure 18 Schematic diagram of the multilayer films 168-0419A and 168-0419B.

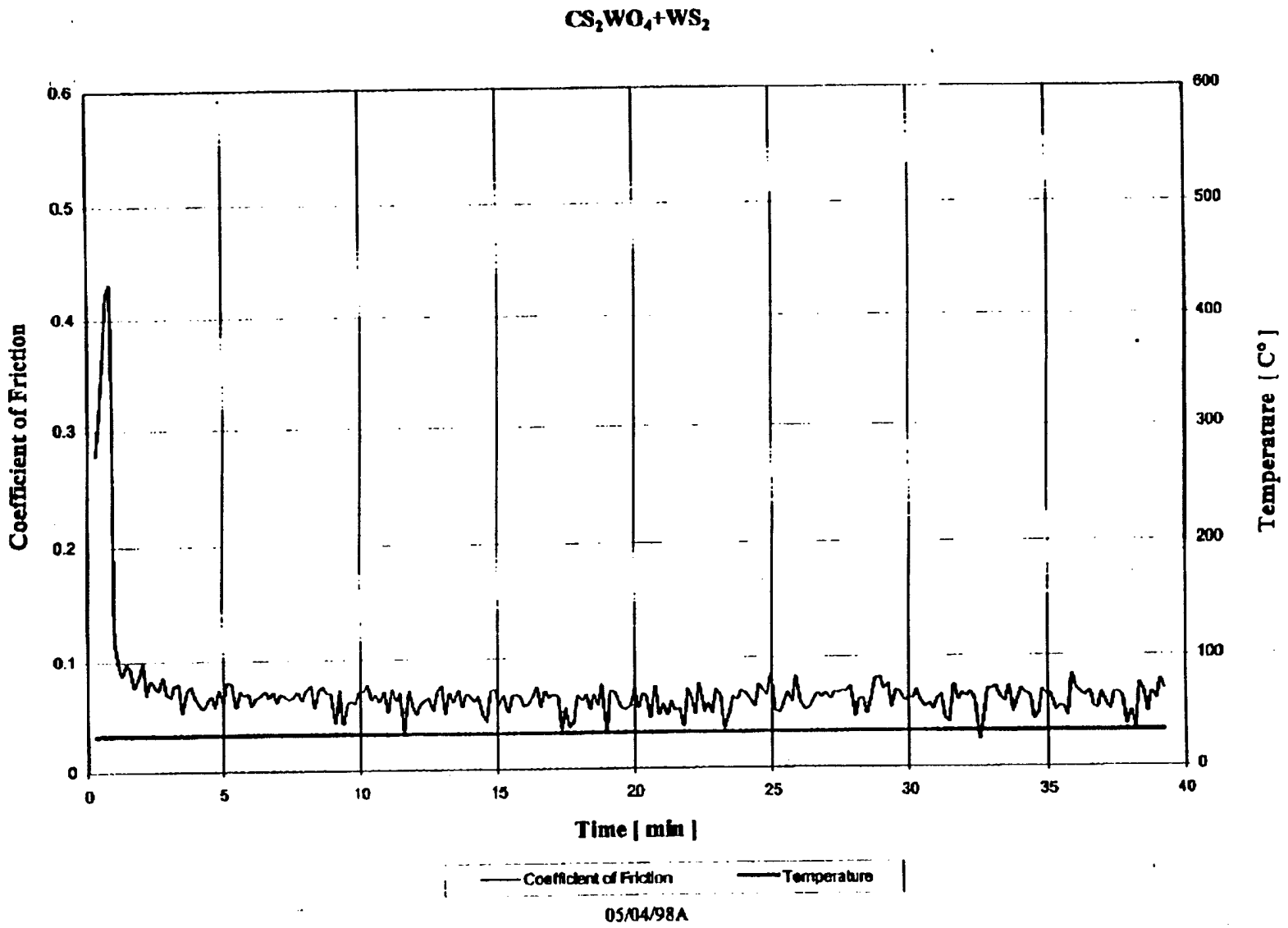

Figure 19a Friction coefficient as a function of time for the sample 168-0419A at room temperature.

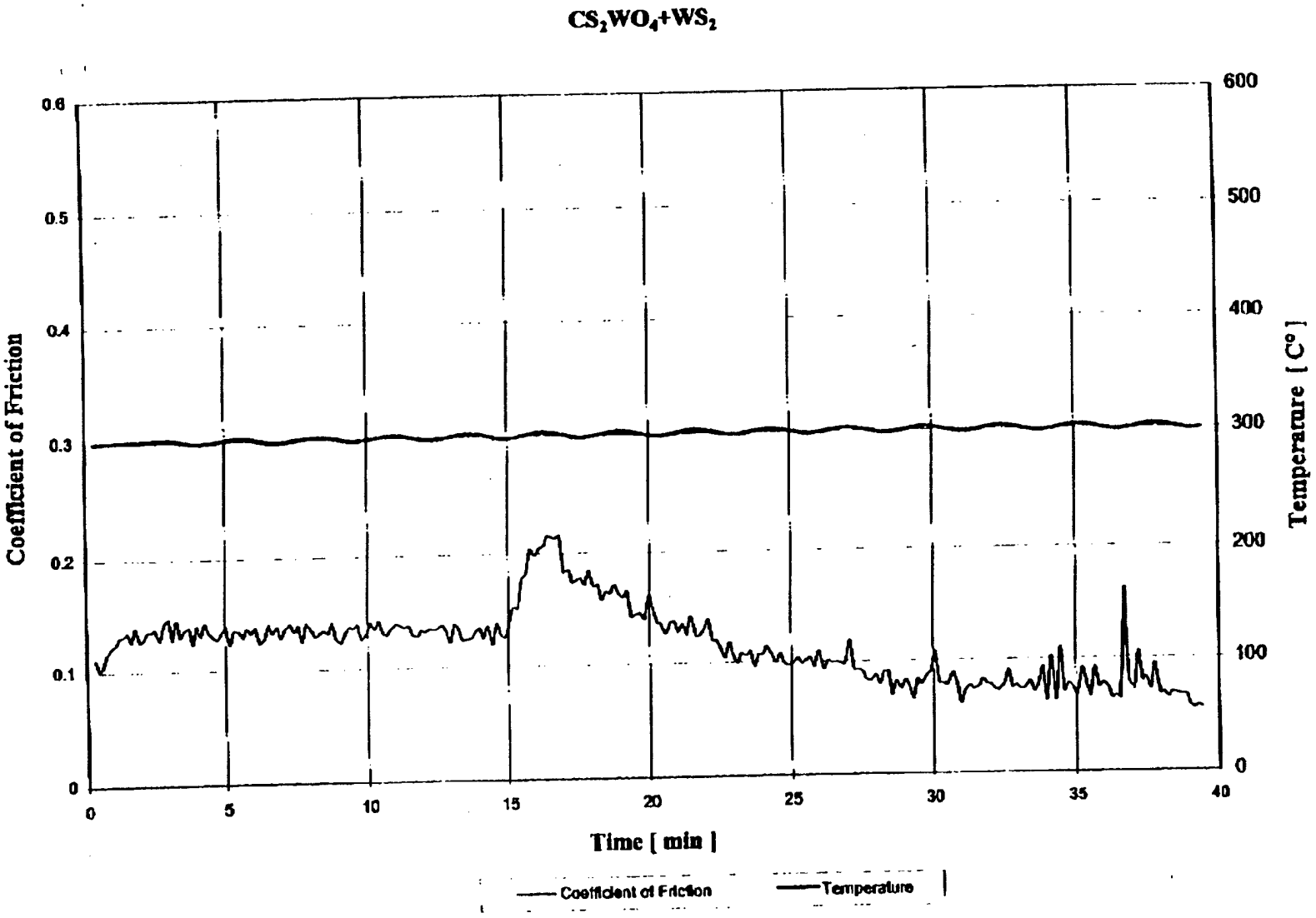

Figure 19b Friction coefficient as a function of time for the sample 168-0419A at 300° C.

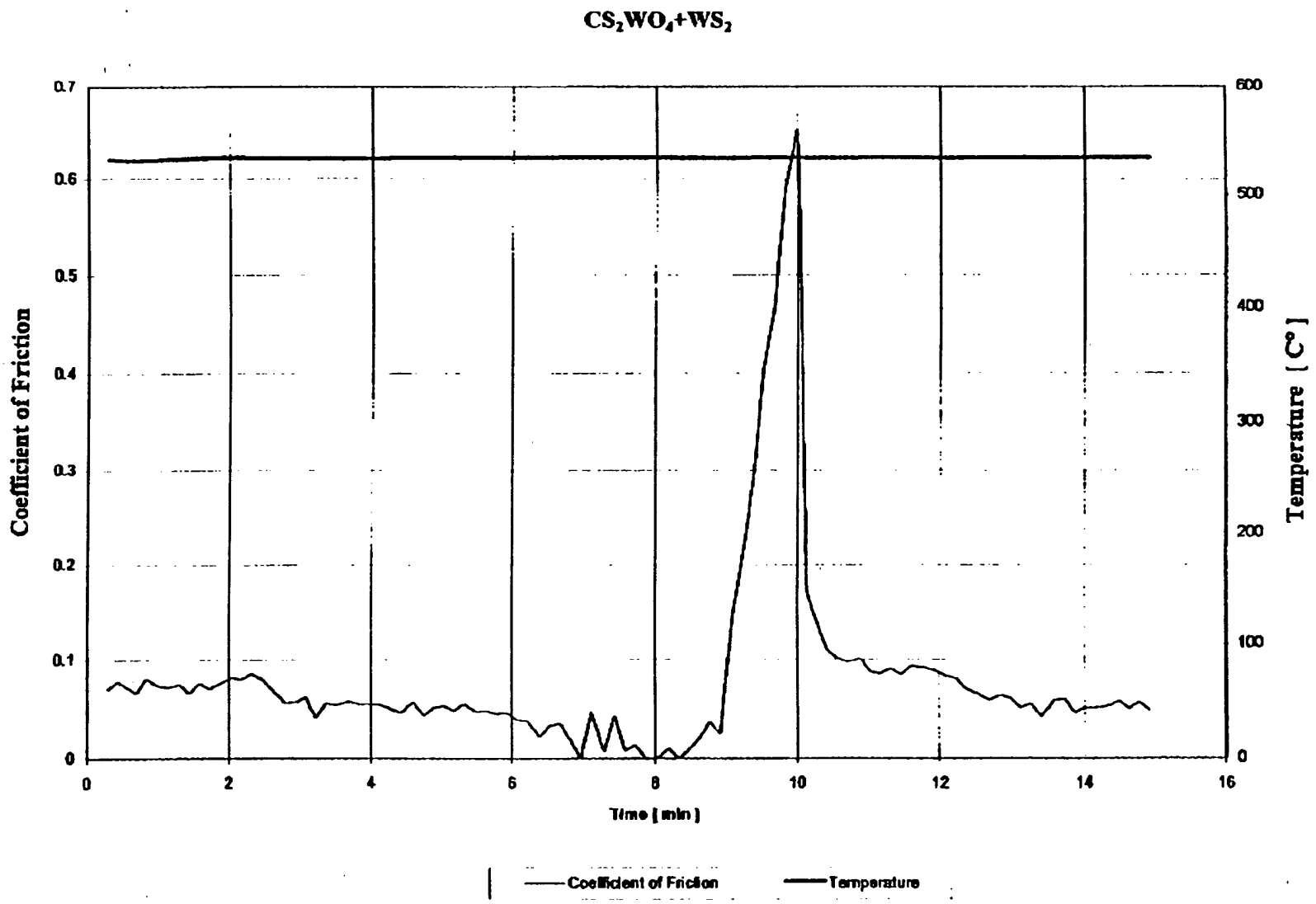

Figure 19c Friction coefficient as a function of time for the sample 168-0419A at 550°C.

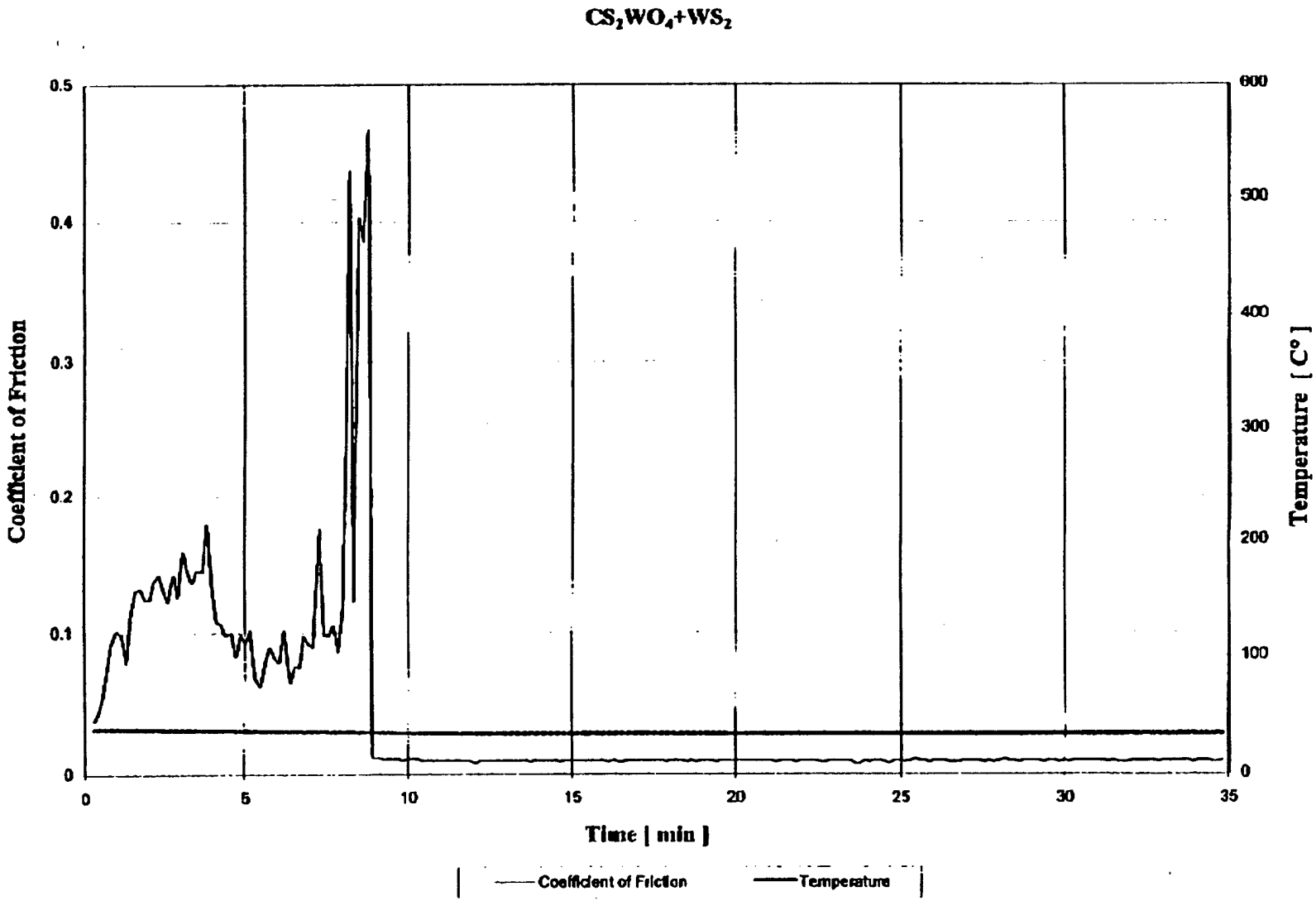

Figure 20a Friction coefficient as a function of time for the sample 168-0419B at room temperature.

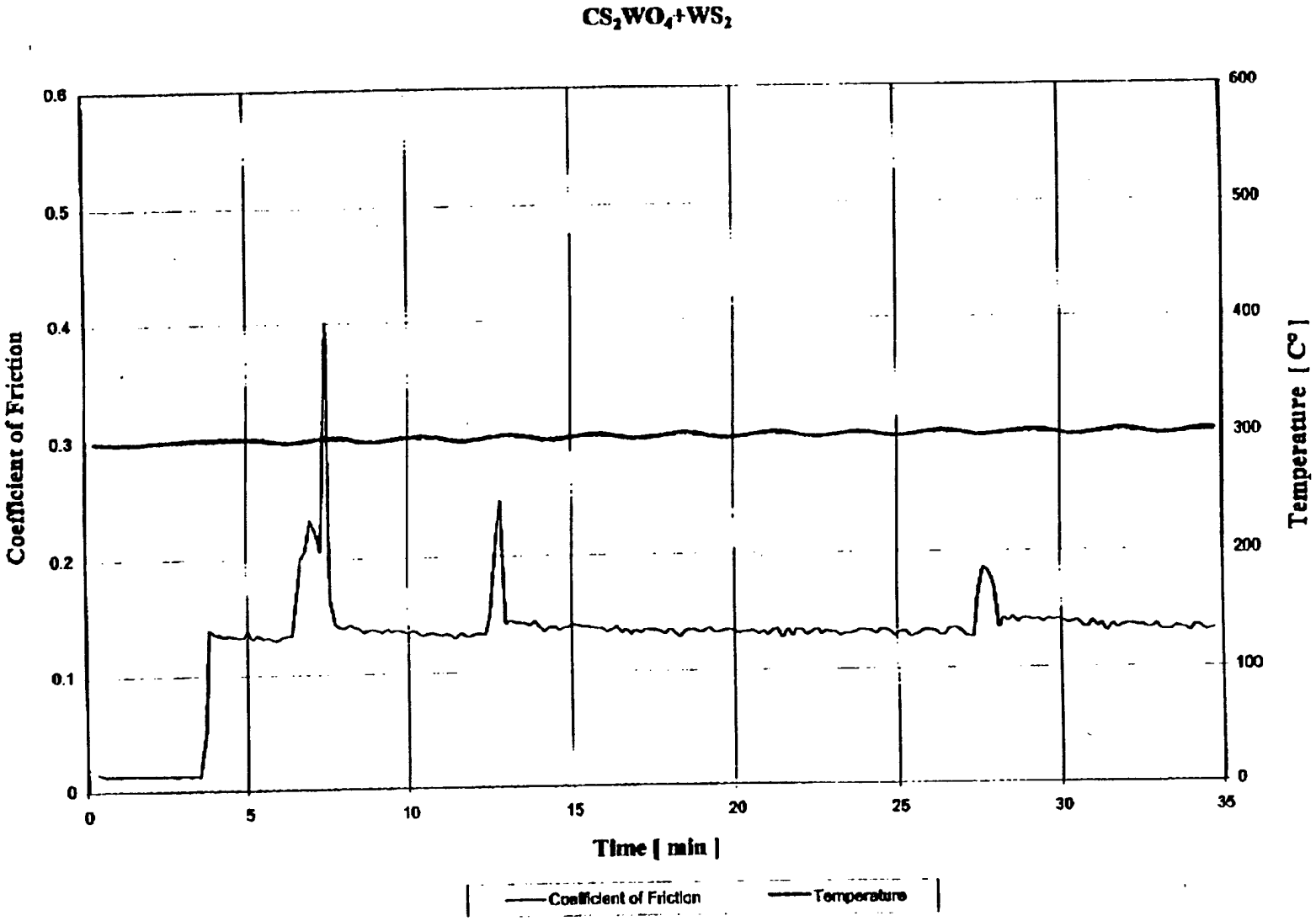

Figure 20b Friction coefficient as a function of time for the sample 168-0419B at 300°C.

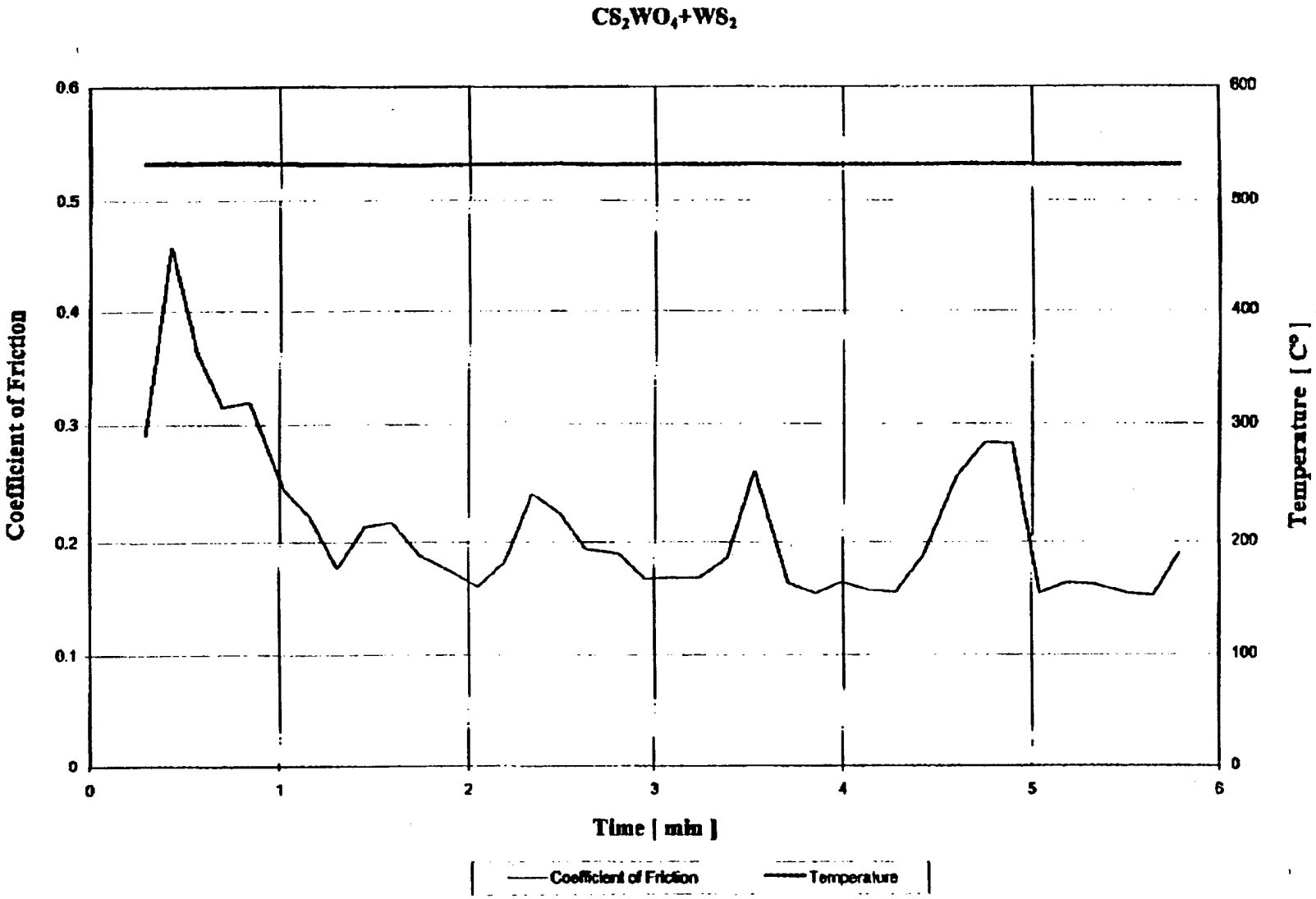

Figure 20c Friction coefficient as a function of time for the sample 168-0419B at 550°C.

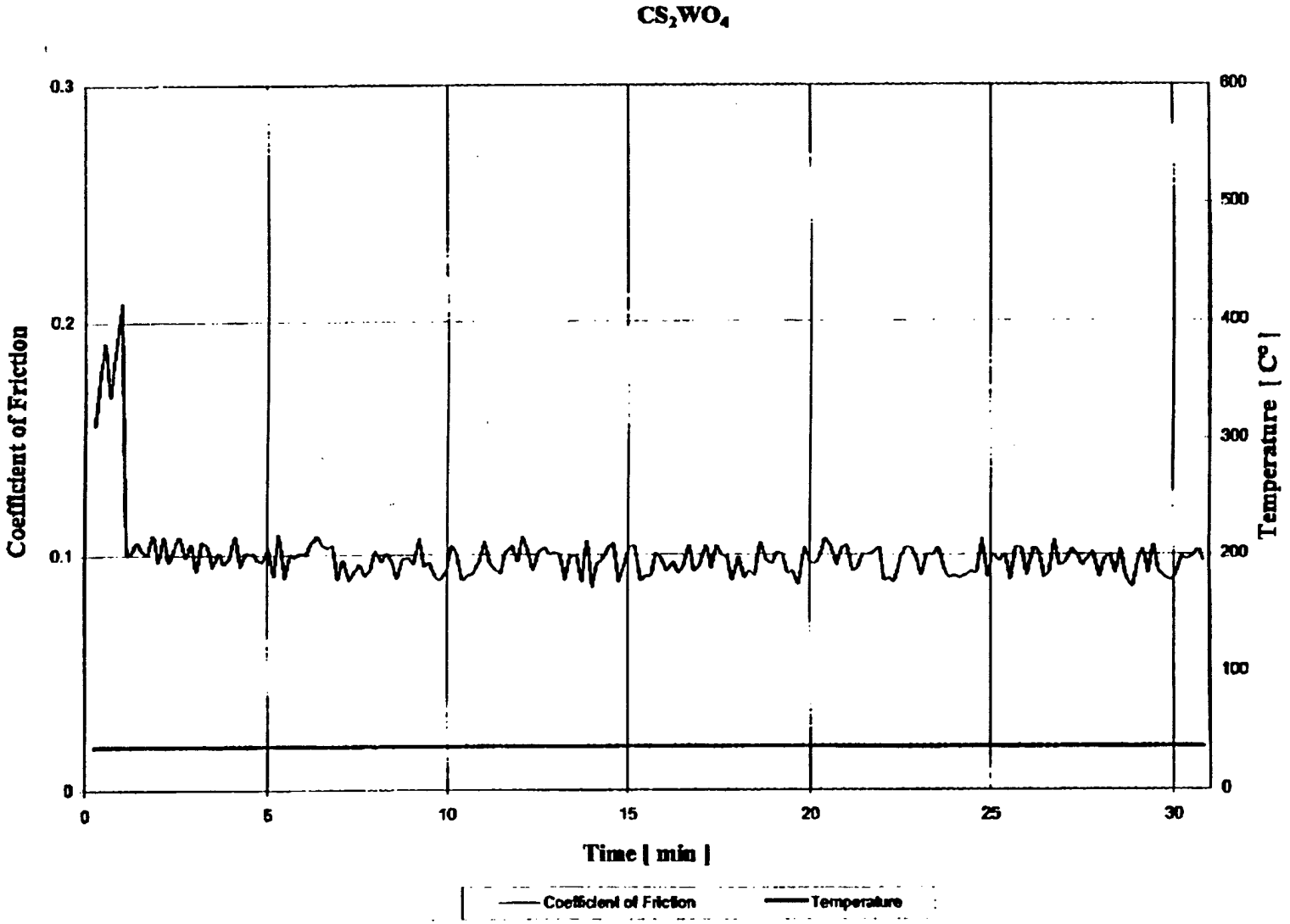

Figure 21a Friction coefficient as a function of time for the Cs_2WO_4 film at room temperature.

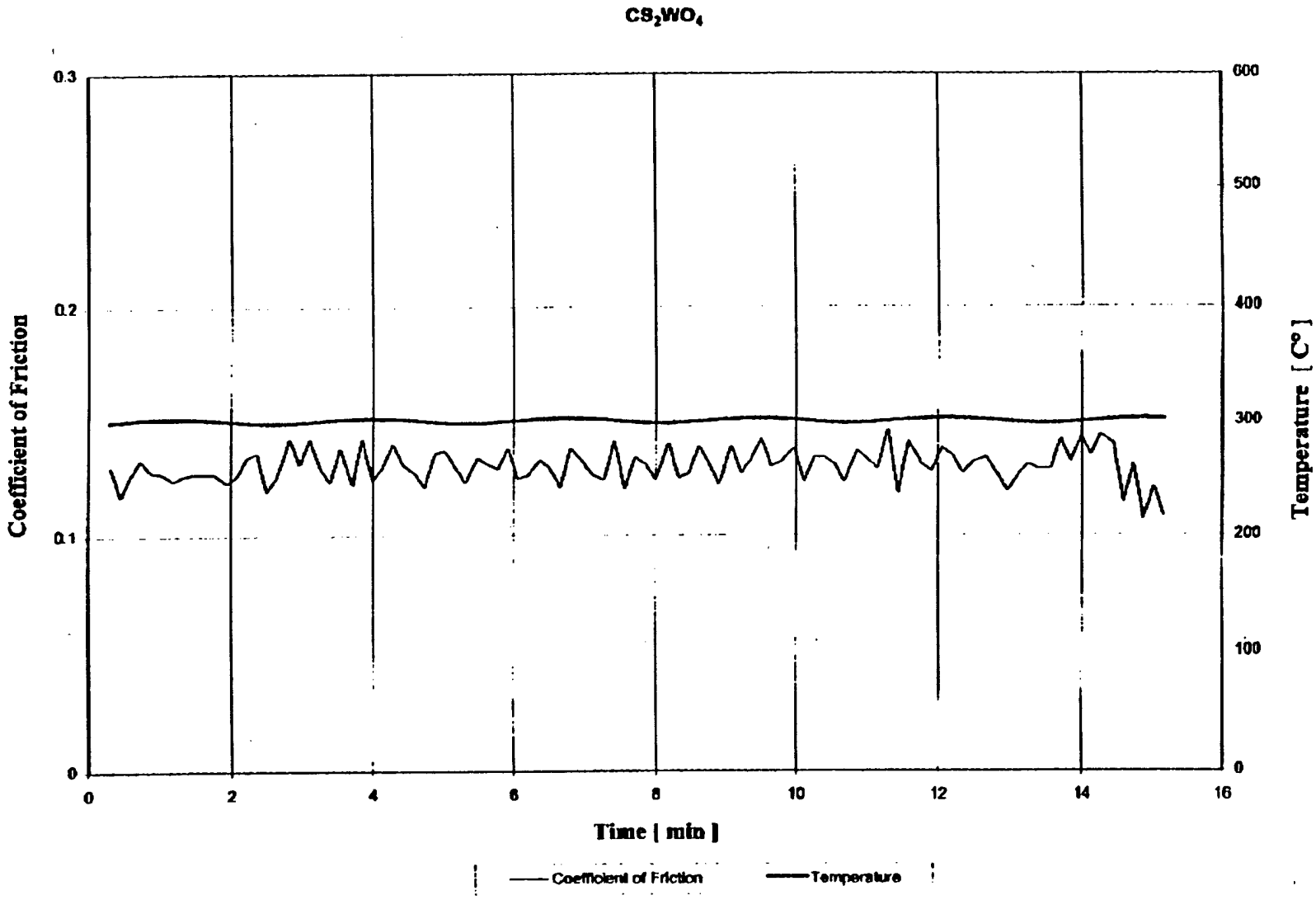

Figure 21b Friction coefficient as a function of time for the Cs_2WO_4 film at 300°C.

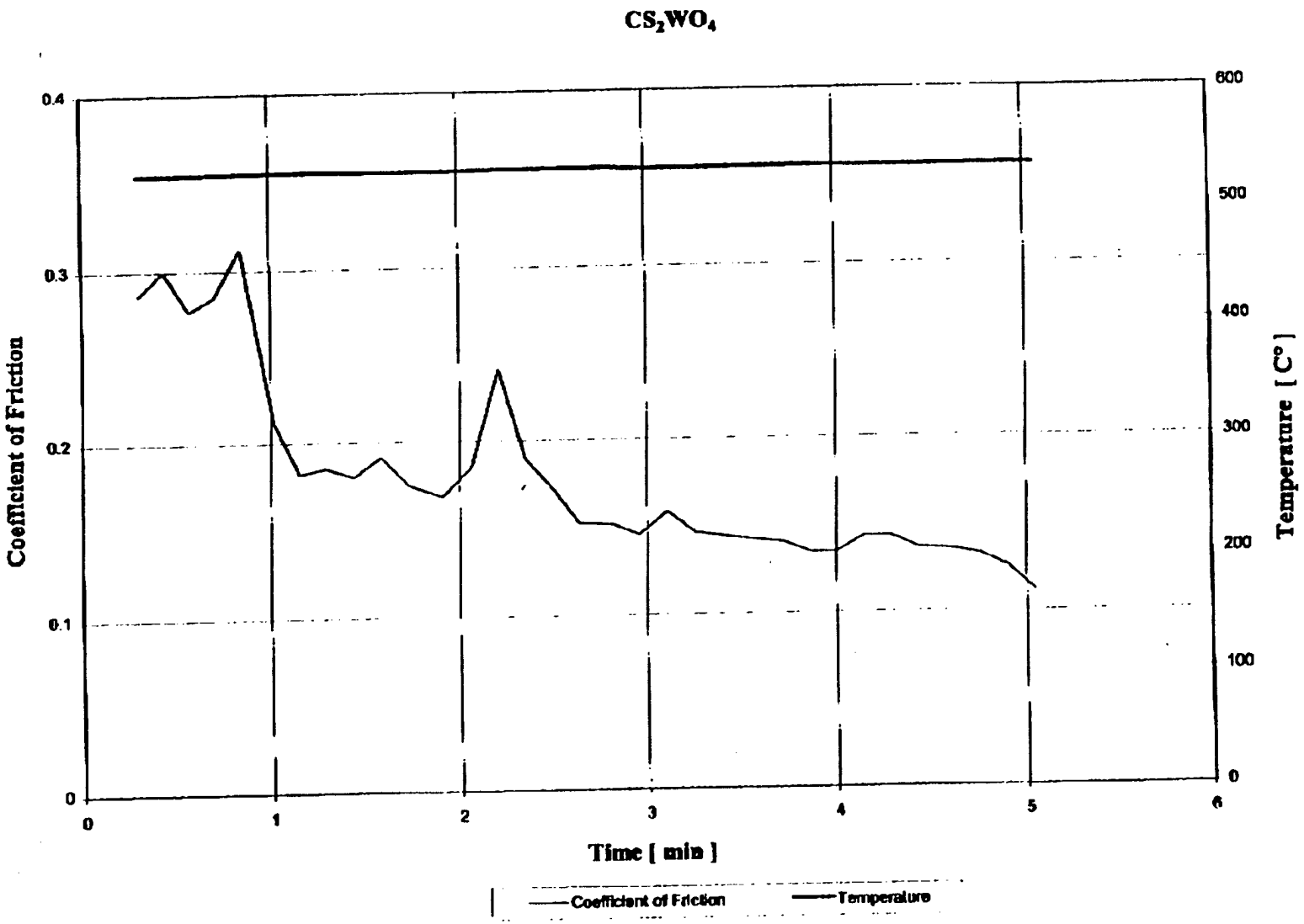

Figure 21c Friction coefficient as a function of time for the Cs_2WO_4 film at 530°C.

U.E.S. 79
(No Lub)

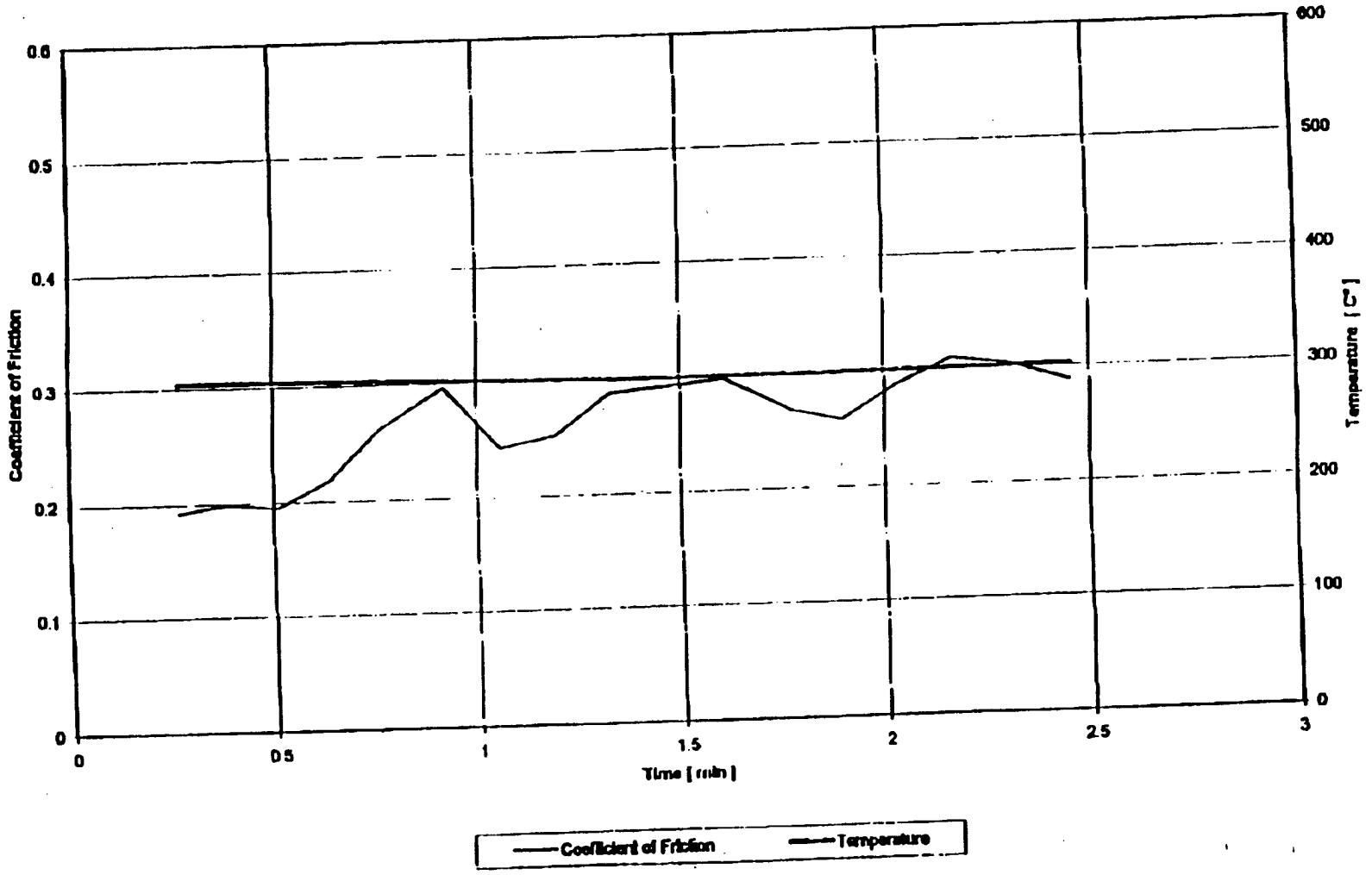

Figure 22a Friction coefficient as a function of time for the Cs_2WOS_3 film at 300°C.

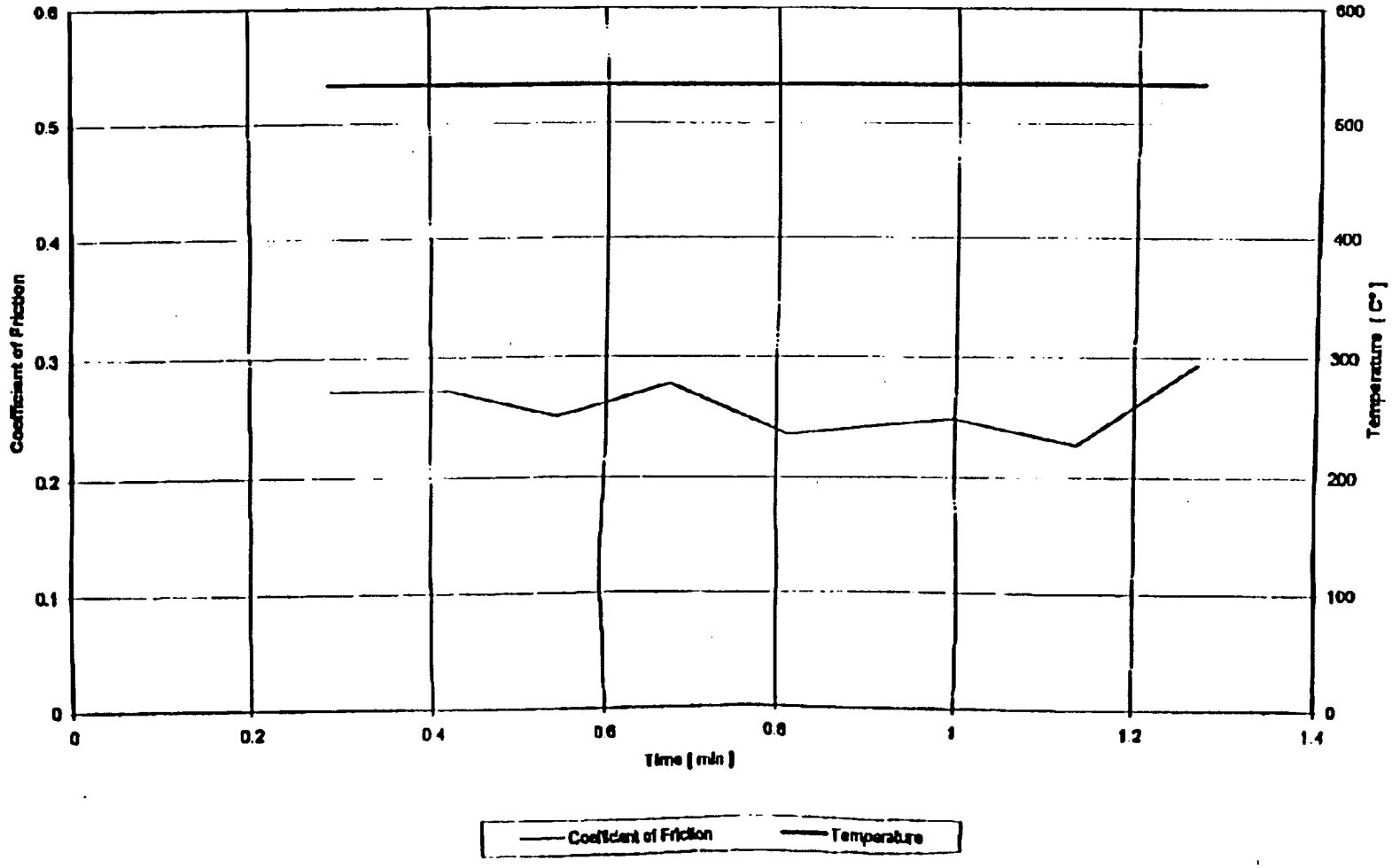

Figure 22b Friction coefficient as a function of time for the Cs_2WOS_3 film at 530°C.